

General Disclaimer

One or more of the Following Statements may affect this Document

- This document has been reproduced from the best copy furnished by the organizational source. It is being released in the interest of making available as much information as possible.
- This document may contain data, which exceeds the sheet parameters. It was furnished in this condition by the organizational source and is the best copy available.
- This document may contain tone-on-tone or color graphs, charts and/or pictures, which have been reproduced in black and white.
- This document is paginated as submitted by the original source.
- Portions of this document are not fully legible due to the historical nature of some of the material. However, it is the best reproduction available from the original submission.

PROPERTIES OF MATERIALS IN HIGH PRESSURE HYDROGEN AT ROOM AND ELEVATED TEMPERATURES



ANNUAL REPORT

Contract NAS8-26191

Prepared for:
George C. Marshall Space Flight Center
National Aeronautics and Space Administration
Marshall Space Flight Center, Alabama 35812



Pratt & Whitney Aircraft
FLORIDA RESEARCH AND DEVELOPMENT CENTER
BOX 2671, WEST PALM BEACH, FLORIDA 33402

**U
A.**
DIVISION OF UNITED AIRCRAFT CORPORATION

CONTENTS

SECTION		PAGE
	ILLUSTRATIONS	iv
	TABLES	vi
I	INTRODUCTION	I-1
II	CONCLUSIONS AND DISCUSSION	II-1
	A. General	II-1
	B. Cast Nickel-Base Alloys	II-1
	C. Wrought Nickel-Base Alloys	II-1
	D. Wrought Cobalt-Base Alloy	II-3
III	MATERIALS AND SPECIMENS	III-1
	A. Test Material	III-1
	B. Test Gases and Material	III-1
	C. Test Specimens	III-4
IV	LOW-CYCLE FATIGUE	IV-1
	A. Conclusions and Discussion	IV-1
	B. Test Procedures	IV-4
V	HIGH-CYCLE FATIGUE	V-1
	A. Introduction	V-1
	B. Conclusions and Discussion	V-1
	C. Test Procedure	V-1
	D. Results	V-5
VI	FRACTURE MECHANICS TESTING	VI-1
	A. Introduction	VI-1
	B. Results and Conclusions	VI-1
	C. Test Procedure	VI-1
VII	CREEP RUPTURE	VII-1
	A. Introduction	VII-1
	B. Results and Conclusions	VII-1
	C. Test Procedure	VII-4
VIII	TENSILE PROPERTIES	VIII-1
	A. Introduction	VIII-1
	B. Conclusions and Discussion	VIII-1
	C. Test Procedure	VIII-11
	D. Results	VIII-11

ILLUSTRATIONS

FIGURE		PAGE
III-1	Typical Microstructure of Materials As-Tested During This Phase of the Program	III-3
III-2	Macrostructure of MAR M-200 DS and IN100 Cast Bars	III-4
III-3	Typical Test Specimens Used to Determine the Effect of High-Pressure Gaseous Hydrogen on Mechanical Properties of Materials	III-5
III-4	Constant Strain Low-Cycle Fatigue Specimen	III-6
III-5	Smooth Axial Fatigue Specimen (High-Cycle Fatigue)	III-7
III-6	Fracture Mechanics Specimen	III-8
III-7	Flat End Creep-Rupture Specimen	III-9
III-8	Ambient-Cryogenic Tensile Specimen (Notch)	III-10
III-9	Ambient-Elevated Temperature Tensile Specimen (Smooth)	III-11
IV-1	Typical Load-Strain Hysteresis Curve Obtained During a Specimen LCF Test	IV-1
IV-2	Low-Cycle Fatigue Life of WASPALOY® at 951°K (1250°F)	IV-3
IV-3	Low-Cycle Fatigue Life of Haynes 188 at 951°K (1250°F)	IV-3
IV-4	Low-Cycle Fatigue Life of IN100 at 951°K (1250°F)	IV-4
V-1	High-Cycle Fatigue Life of MAR M-200 DS at 1250°F	V-2
V-2	Typical MAR M-200 DS Cross Section Adjacent to Fracture Face (Mag: 100X)	V-2
V-3	High-Cycle Fatigue Life of IN100 at 1250°F	V-3
V-4	Macrograph of IN100 Test Specimen Showing Excessive Micro Shrinkage at Fracture Face (Mag: 10X)	V-3
VI-1	Cyclic Flaw Growth Data for AMS 5706 WASPALOY®	VI-2
VI-2	Sustained-Load Flaw Growth Data for AMS 5706 WASPALOY®	VI-2
VI-3	Tensile Machine, Test Environment Controls, and Data Acquisition Equipment Located in the Blockhouse	VI-3
VI-4	High-Pressure Gaseous Environment Fracture Toughness Test Vessel Installed on Tensile Machine in the Test Cell	VI-4

ILLUSTRATIONS (Continued)

FIGURE		PAGE
VII-1	Stress Rupture of WASPALOY [®] (AMS 5706) at 951°K (1250°F)	VII-2
VII-2	Stress Rupture of Astroloy at 951°K (1250°F)	VII-2
VII-3	Stress Rupture of Haynes 188 at 951°K (1250°F)	VII-3
VII-4	Stress Rupture of IN100 at 951°K (1250°F)	VII-3
VII-5	Micrographs From Gage Section of an Astroloy Creep- Rupture Specimen Tested at 951°K (1250°F) in 34.5-MN/m ² (5000-psig) Gaseous Hydrogen	VII-5
VII-6	Creep-Rupture of WASPALOY [®] (AMS 5706) at 951°K (1250°F)	VII-6
VII-7	Creep-Stress Rupture of Astroloy at 951°K (1250°F)	VII-6
VII-8	Creep-Rupture Water Injection System	VII-8
VIII-1	Tensile Properties of MAR M-200 DS in 34.5-MN/m ² (5000-psig) Gaseous Environment at 300°K (80°F) and 951°K (1250°F)	VIII-3
VIII-2	Tensile Properties of IN100 in 34.5-MN/m ² (5000-psig) Gaseous Environment at 300°K (80°F) and 951°K (1250°F)	VIII-4
VIII-3	Tensile Properties of WASPALOY [®] in 34.5-MN/m ² (5000-psig) Gaseous Environment at 951°K (1250°F)	VIII-5
VIII-4	Effect of Temperature on Notched ($K_t = 8.0$) Tensile Strength of Astroloy at 3.45 MN/m ² (5000 psig)	VIII-7
VIII-5	Effect of Temperature on Notched ($K_t = 8.0$) Tensile Strength of Astroloy at 34.5 MN/m ² (5000 psig)	VIII-7
VIII-6	Effect of Temperature on Smooth Tensile Yield and Ultimate Strength of Astroloy at 3.45 MN/m ² (5000 psig)	VIII-8
VIII-7	Effect of Temperature on Smooth Tensile Ductility of Astroloy at 3.45 MN/m ² (5000 psig)	VIII-8
VIII-8	Micrographs From Gage Section of an Astroloy Tensile Specimen Tested at 1144°K (1600°F) in 3.45-MN/m ² (500-psig) Helium	VIII-9
VIII-9	Micrographs From Gage Section of an Astroloy Tensile Specimen Tested at 1144°K (1600°F) in 3.45-MN/m ² (500-psig) Hydrogen	VIII-10

TABLES

TABLE		PAGE
I-1	Test Program Showing Type of Tests and Test Conditions Used to Determine the Susceptibility of Various Alloys to Environmental Hydrogen Embrittlement or Degradation	I-2
III-1	Materials For Hydrogen Degradation Testing	III-2
III-2	Specimens Tested to Determine Effect of High-Pressure Gaseous Hydrogen Upon Mechanical Properties	III-5
IV-1	Elevated Temperature, Low-Cycle Fatigue Properties in High-Pressure Gaseous Environment	IV-2
V-1	Elevated-Temperature, High-Cycle Fatigue Properties of Materials in High-Pressure Gaseous Environments	V-6
VII-1	Degradation Based on Rupture Life	VII-1
VII-2	Creep-Rupture Properties of Materials in High-Pressure Gaseous Environment	VII-9
VIII-1	Relative Degradation of Tensile Properties of Materials in Gaseous Hydrogen Environment	VIII-2
VIII-2	Tensile Properties of Materials in High-Pressure Gaseous Environment	VIII-12

SECTION I INTRODUCTION

This report is submitted in accordance with the requirements of Contract NAS8-26191 and represents the second annual report covering the period 29 June 1971 to 30 June 1972. Results of efforts for the previous year were reported in PWA FR-4566. (1) Experimental efforts in this program for this period have consisted of mechanical property tests of wrought and cast nickel-base alloys and one wrought cobalt-base alloy in 34.5-MN/m² (5000-psig) helium and hydrogen or hydrogen mixtures and the comparison of test results to determine degradation of properties due to the hydrogen environments. The testing program for this year's work on this contract is outlined in table I-1.

All testing was conducted on solid specimens exposed to external gaseous pressure. Specific mechanical properties determined and the testing methods used are summarized below:

- Low-Cycle Fatigue - Low-cycle fatigue life was established by constant total-strain testing using smooth specimens and closed-loop testing machines.
- High-Cycle Fatigue - High-cycle fatigue life was established by load (stress) controlled tension-tension testing using smooth specimens and servo-actuated, closed-loop machines.
- Fracture Mechanics - Fracture toughness, threshold stress intensity, and cyclic stress intensity were determined using center-notched, fatigue-precracked, plate specimens.
- Creep-Rupture - Creep rate and time to failure were determined using smooth specimens and a standard creep-rupture machine equipped with a recording extensometer.
- Tensile - Smooth and notched tensile tests were conducted on solid specimens using ASTM tensile testing techniques.

This report is arranged in sections, which cover the program conclusions, materials tested, and results and conclusions of the individual property tests.

This program has been conducted using the Program Manager - Project Group System by the Pratt & Whitney Aircraft, Florida Research and Development Center, Materials Development Laboratory, under the cognizance of Mr. W. B. McPherson, Materials Division, Astronautics Laboratory, Marshall Space Flight Center.

(1) "Properties of Materials in High Pressure Hydrogen at Cryogenic, Room, and Elevated Temperatures," Annual Report, Contract NAS8-26191, PWA FR-4566, dated 30 June 1971.

Table I-1. Test Program Showing Type of Tests and Test Conditions Used to Determine the Susceptibility of Various Alloys to Environmental Hydrogen Embrittlement or Degradation

Type of Tests													
	Temperature,		Pressure		Environment	Low-Cycle Fatigue	High-Cycle Fatigue	Creep-Rupture	Fracture Toughness	Threshold Stress Intensity	Cyclic Stress Intensity	Smooth Tensile	Notched Tensile
	°K	°F	MN/m ²	psig									
MAR-M-200 DS	300	80	34.5	5000	Hydrogen							X	
	300	80	34.5	5000	Helium							X	
	951	1250	34.5	5000	Hydrogen		X					X	
	951	1250	34.5	5000	Helium		X					X	
IN100	300	80	34.5	5000	Hydrogen							X	
	300	80	34.5	5000	Helium							X	
	951	1250	34.5	5000	Hydrogen	X	X	X				X	
	951	1250	34.5	5000	Helium	X	X	X				X	
WASPALLOY [®]	300	80	34.5	5000	Hydrogen				X	X			
	300	80	34.5	5000	Helium				X				
	951	1250	34.5	5000	Hydrogen	X		X				X	
	951	1250	34.5	5000	Helium	X		X				X	
Astroloy	300	80	3.45	500	Hydrogen								X
	300	80	3.45	500	Helium								X
	951	1250	3.45	500	Hydrogen								X
	951	1250	3.45	500	Helium								X
	1144	1600	3.45	500	Hydrogen							X	X
	1144	1600	3.45	500	Helium							X	X
Haynes 188	951	1250	34.5	5000	Hydrogen			X					X
	951	1250	34.5	5000	Helium	X		X					X
	951	1250	34.5	5000	Hydrogen and Water								X

Acknowledgement is given to the following personnel of the Project Group:

Mr. J. L. Bearden	- High-Cycle Fatigue Testing
Mr. R. B. Bogard	- Low-Cycle Fatigue Testing
Mr. J. Doyle	- Tensile Testing
Mr. J. E. Gies	- Test Support, Rocket Test Facility
Mrs. A. F. Kirkpatrick	- Proposal and Report Efforts
Mr. T. M. Pruitt	- Test Support, Rocket Test Facility
Mr. J. F. Schratt	- Creep-Rupture Testing
Mrs. C. B. Stevens	- Metallurgical Investigation
Mr. D. J. Stoddard	- Cost and Planning Efforts
Mr. B. H. Walker	- Fracture Mechanics Testing
Miss M. Zaccagnino	- Proposal and Report Efforts

SECTION II CONCLUSIONS AND DISCUSSION

A. GENERAL

The efforts in this program for this period have consisted of conducting fatigue, fracture mechanics, creep-rupture, and tensile tests on two cast nickel-base alloys (MAR M-200 DS and IN100), two wrought nickel-base alloys (WASPALLOY[®] and Astroloy), and one wrought cobalt-base alloy (Haynes 188) to determine the susceptibility of these alloys to environmental hydrogen embrittlement or degradation.

Detailed conclusions are presented in the various sections pertaining to type of test. General conclusions, as pertaining to the various alloys, are presented below:

B. CAST NICKEL-BASE ALLOYS

Tested were MAR M-200 DS (PWA 664) and IN100 (PWA 658).

The low-cycle and high-cycle fatigue properties, both strain controlled and tension-tension load controlled, were degraded for both alloys tested at 951°K (1250°F) in 34.5-MN/m² (5000-psig) hydrogen as compared to similar conditions in helium.

The stress-rupture life of IN100 at 951°K (1250°F) was extremely degraded by the 34.5-MN/m² (5000-psig) hydrogen. The rupture life of IN100 at 551-MN/m² (80-ksi) stress was greater than 140 hr (test discontinued) in helium in comparison to 1.6 hr in hydrogen at the same stress, gas pressure, and temperature.

The tensile properties, 0.2% yield, ultimate, elongation and reduction in area, were evaluated at 300°K (80°F) and 951°K (1250°F) and 34.5-MN/m² (5000-psig) hydrogen or helium pressure. Ductility (elongation and reduction in area) of both alloys was the most affected by the hydrogen, with as much as 75% decrease in ductility at 300°K (80°F). The degree of degradation of both alloys decreased at 951°K (1250°F), with IN100 significantly less degraded in hydrogen at elevated temperature of 951°K (1250°F) than at 300°K (80°F).

C. WROUGHT NICKEL-BASE ALLOYS

Tested were WASPALLOY (AMS 5706) and Astroloy (PWA 1013).

The low-cycle fatigue (LCF) life of WASPALLOY at 34.5-MN/m² (5000-psig) pressure hydrogen had only slight indications of degradation at 951°K (1250°F). Previous LCF data reported by VanWanderham, M., and Harris, J. A., Jr.,¹

¹VanWanderham, M. C., and Harris, J. A., Jr., "Low-Cycle Fatigue of Metals in High-Pressure Gaseous Hydrogen at Cryogenic Ambient and Elevated Temperatures," presented to the 1971 WESTEC Conference, Los Angeles, California.

Pratt & Whitney Aircraft

PWA FR-5129

on Waspaloy at 34.5-MN/m^2 (5000-psig) pressure hydrogen or helium showed much more hydrogen degradation at both 80°F and 540°F . However, this degree of degradation does not present itself at 951°K (1250°F). Astroloy was not tested in LCF.

Creep and rupture properties of both Waspaloy and Astroloy were degraded in 34.5-MN/m^2 (5000-psig) hydrogen at 951°K (1250°F) as compared to similar conditions in helium. Rupture life of Waspaloy in 34.5-MN/m^2 (5000-psig) hydrogen pressure at 951°K (1250°F) and stress of 607 MN/m^2 (88 ksi) was 25.1 hr in comparison to similar conditions in helium of 58.2 hr - a degradation of 57%. Similar test conditions, except stress of 793 MN/m^2 (115 ksi), for Astroloy produced 59.6 hr to rupture in hydrogen compared to 87.8 hr in helium. Generally, the creep rates were greater in hydrogen than helium for both Waspaloy and Astroloy.

Significantly lower fracture toughness values for Waspaloy occurred at 300°K (80°F) in 34.5-MN/m^2 (5000 psig) hydrogen as compared to helium. Fracture toughness values of approximately $70\text{ MN/m}^2\sqrt{\text{m}}$ (62 ksi $\sqrt{\text{in.}}$) occurred in hydrogen in comparison to $103\text{ MN/m}^2\sqrt{\text{m}}$ (93 ksi $\sqrt{\text{in.}}$) in helium. An initial stress intensity K_{Ii} of $27.9\text{ MN/m}^2\sqrt{\text{m}}$ (25 ksi $\sqrt{\text{in.}}$) is required for 100-cycle life, and a sustained-load threshold stress intensity K_{TH} of $33\text{ MN/m}^2\sqrt{\text{m}}$ (30 ksi $\sqrt{\text{in.}}$) yields no flaw growth in 100 hr at 300°K (80°F) and 34.5-MN/m^2 (5000-psig) hydrogen pressure.

Tensile tests of smooth specimens were conducted on Waspaloy at 951°K (1250°F) and 34.5-MN/m^2 (5000-psig) hydrogen or helium pressure. Degradation was noted in percent elongation only, and no degradation was noted in yield and ultimate strengths or reduction of area.

The Astroloy material was tested at two pressure levels, 3.45 and 34.5 MN/m^2 (500 and 5000 psig) and three temperatures, 300° , 951° , and 1144°K (80° , 1250° , and 1600°F). Notched ($K_t = 8.0$) tensile strength was most extensively evaluated, being determined at each of three temperatures at two pressures. Effects of the hydrogen environment were more pronounced at 34.5 MN/m^2 (5000 psig) than at 3.45 MN/m^2 (500 psig). At 34.5 MN/m^2 (5000 psig), notched tensile strength degradation was approximately twice that at 3.45 MN/m^2 (500 psig) for temperatures of 300° and 951°K (80° and 1250°F). The general decrease in notched strength with increasing temperature was expected, as well as the decrease in amount of hydrogen degradation with increasing temperature. However, at 1144°K (1600°F), higher properties in hydrogen were observed than in helium. Additional testing was conducted, which verified this occurrence. Metallographic examination of failed specimens tested at 1144°K (1600°F) in helium and hydrogen could not provide definite reasons for this property reversal. The most significant difference between the hydrogen and helium specimens was the occurrence of voids at large unsoluted gamma prime particles located completely within a grain. These intragranular voids, while not consistent from specimen to specimen, occurred only in specimens tested in the hydrogen environment and not in specimens tested in the helium environment. The significance of this difference is not understood. At elevated temperatures, particularly those temperatures above 1033°K (1400°F), several factors can contribute to the response of Astroloy (or other nickel-base alloys) in the helium and hydrogen environments. The

hydrogen will disassociate from a molecular to atomic gas with both the physical and chemical activity of the hydrogen atoms at a very high level; therefore, diffusion can proceed at a high rate. The 1144°K (1600°F) temperature is beyond the normal operating range for Astroloy. In fact, this temperature is in the range of the aging heat treatment temperatures, and structural changes can take place even during the short time exposures of a tensile test, because of the high straining that is occurring. To explain this change in degree of degradation, and particularly the reversal of helium and hydrogen properties at 1144°K (1600°F), a better understanding of the hydrogen-material interaction mechanism must be obtained.

D. WROUGHT COBALT-BASE ALLOY

Tested was Haynes 188 (PWA 1015).

The low-cycle fatigue life of Haynes 188 at 34.5-MN/m² (5000-psig) pressure hydrogen was slightly degraded at 951°K (1250°F). The degree of degradation was less than previously reported by VanWanderham, M., and Harris, J. A. Jr., on Haynes 188 tested at 300°K (80°F) and 34.5-MN/m² (5000-psig) hydrogen pressure. Therefore, it may be concluded that the degree of hydrogen degradation on LCF life decreases with increased temperature.

The stress-rupture life of Haynes 188 at 951°K (1250°F) was degraded by the 34.5-MN/m² (5000-psig) hydrogen or hydrogen/water vapor as compared to helium pressure at same stress, temperature, and pressure condition. At a stress of 365 MN/m² (53 ksi), the life to rupture was 80.3, 43.2, and 55.5 hr for helium, hydrogen, and hydrogen/water vapor, respectively. Generally, the creep rates were greater in hydrogen than helium at 951°K (1250°F) and 34.5-MN/m² (5000-psig) gas pressure.

SECTION III MATERIALS AND SPECIMENS

A. TEST MATERIAL

The purpose of this contract is to determine the susceptibility to hydrogen degradation of various alloys proposed for use in the hydrogen environments of spacecraft. This report describes the second year achievements of this program. Previous effort, reported in PWA FR-4566, evaluated seven wrought nickel-, iron-, and titanium-base alloys. For this phase, wrought and cast nickel-base and wrought cobalt-base alloys were tested. Table III-1 lists the materials and conditions in which they were received and tested.

The cast bars of MAR M-200 DS and IN100 were received as-cast and were judged radiographically sound before being heat treated. Barstock of WASPALOY[®] and Haynes 188 was received in the solution-annealed condition. Specimen blanks were cut from the barstock materials and, in the case of the WASPALOY, subsequent heat treatment performed. The Astroloy material was procured as a pancake forging and was fully heat treated in this configuration prior to cutting specimen blanks. Specimen blanks were oriented with their axis in the circumferential direction and were taken from the periphery of the forging. Typical microstructures of each material in the as-tested condition are shown in figure III-1.

Macroetched bars of the MAR M-200 DS and IN100 cast materials are shown in figure III-2. Microstructures were acceptable with some microshrinkage evident in the cast MAR M-200 DS and IN100 material. This microshrinkage was within the intent of the purchasing specifications. As no industry standard specifications for these materials have been established, acceptable microshrinkage levels are based upon experience with gas turbine engine thin-wall castings. Metallurgical examination of some specimens that produced questionable test results did reveal excessive microshrinkage and/or porosity at or near the fracture surfaces. In these cases, retests were conducted.

B. TEST GASES AND MATERIAL

Helium and hydrogen were used during the testing of specimens, and nitrogen was used as a preliminary purge gas. Hydrogen was provided under Military Specification P-27201A, which requires the gas to have an oxygen content of less than 1 part per million (1 ppm). Analysis verified gas supply to be of this purity. Other aspects of test gas handling and sampling were as discussed in PWA FR-4566.

Mixtures of hydrogen and water were used in performing some of the creep-rupture testing. De-ionized water was prepared for injection into the vessel by distillation to remove dissolved gases and then establishing a partial vacuum over the water. The water container is sealed and installed in the hydrogen supply system, which injects the water into a container in the chamber positioned to enable vaporization by furnace heat. Details of the injection system and procedure are described in Section VII, Creep-Rupture.

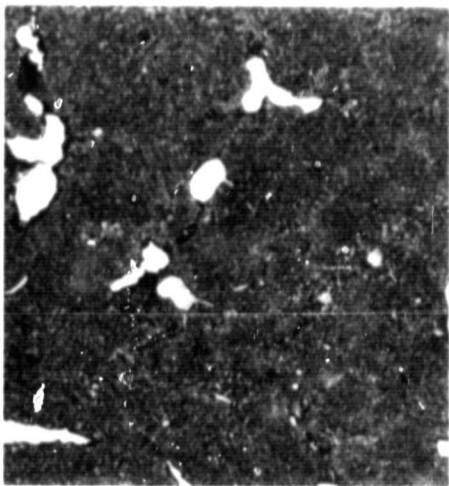
Table III-1. Materials For Hydrogen Degradation Testing

Name	Base	Form	Purchasing Specification	Heat Code	As-Received Condition	As-Tested Condition
MAR M-200DS	Nickel	Cast	PWA 664	P-9108	Cast Bars 139.7 mm by 12.7 mm Diameter 155.5 mm by 19.05 mm Diameter	Heat Treated: 1477°K, 2 hr, Air Cool 1144°K, 32 hr, Air Cool
IN100	Nickel	Cast	PWA 658	P-924S	Cast Bars 139.7 mm by 12.7 mm Diameter 155.5 mm by 19.05 mm Diameter	Heat Treated: 1144°K, 12 hr, Air Cool
WASPALLOY®	Nickel	Wrought	AMS 5706 AMS 5706	L1288K13 BWKJ	19.05-mm Diameter Barstock 50.8-mm by 10.16-mm Thick Barstock	Heat Treated: 1293°K, 4 hr, Oil Quench 1116°K, 4 hr, Air Cool 1033°K, 4 hr, Air Cool
Astroloy	Nickel	Wrought	PWA 1013	LKKC	447.0-mm Diameter by 41.9-mm Thick Pancake Forging	Heat Treated: 1380°K, 4 hr, Oil Quench 1144°K, 8 hr, Air Cool 1255°K, 4 hr, Air Cool 922°K, 24 hr, Air Cool 1033°K, 8 hr, Air Cool
Haynes 188	Cobalt	Wrought	PWA 1015	YFYR	12.7-mm and 15.87-mm Diameter Barstock	Heat Treated: 1450°K, 30 min, Air Cool

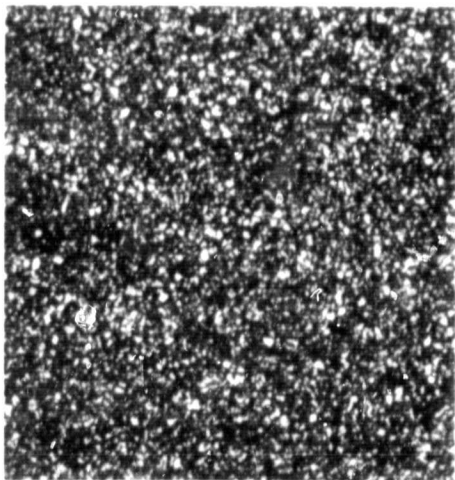
NOTE: 1. Spectrographic Analysis Verified Materials
2. Material Met Requirements of Purchasing Specifications.



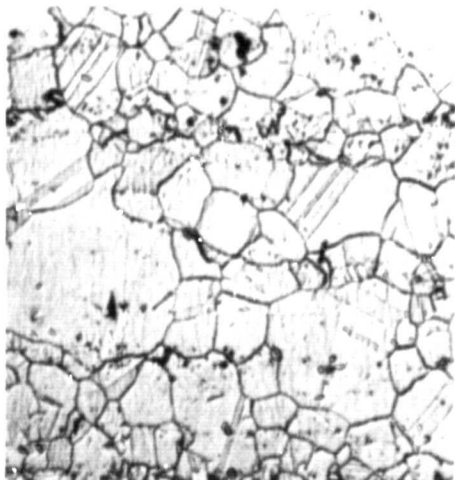
FAM 76856
MAR M-200 DS



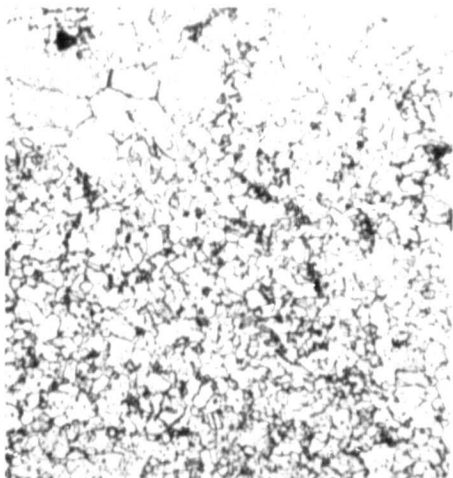
FAM 76855
IN100



FAM 76857
WASPALOY®



FAM 76874
WASPALOY®
(Fracture Mechanics Specimens)



FAM 70970
ASTROLOY



FAM 76858
HAYNES 188

MAG: 100X

Figure III-1. Typical Microstructure of
Materials As-Tested During
This Phase of the Program

FD 62085

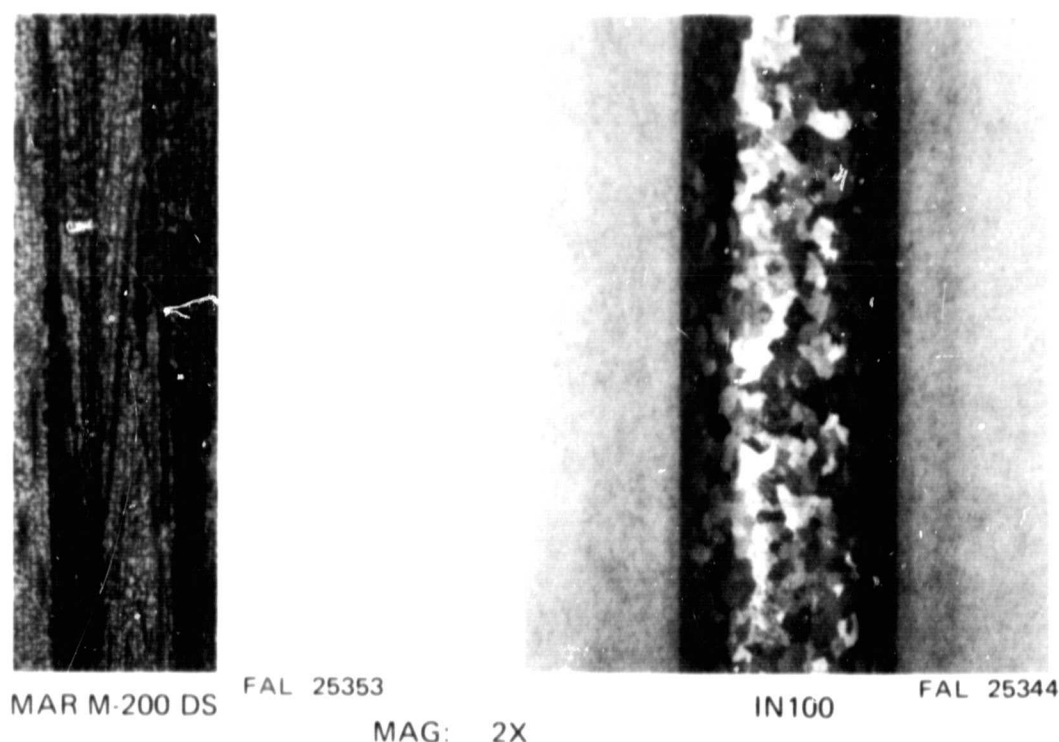


Figure III-2. Macrostructure of MAR M-200 DS and IN100 Cast Bars

C. TEST SPECIMENS

Specimens used for this phase of the contract were identical to those reported in PWA FR-4566, except for the fracture mechanics specimens. Surfaces of all specimens were machined and finished to an average roughness of $16 \mu\text{in. RMS}$ or less. Gage sections of specimens were polished prior to testing. The notch used for tensile specimens to obtain a stress concentration factor of 8.0 was designed according to Peterson¹ and machined by grinding. Smooth tensile specimens had a gage section diameter of 6.37 mm. The fracture mechanics specimen was of the center slot (or notch) type, with a thickness of 2.54 mm. The slot was machined into the specimen by use of electrical discharge machining (ELOX). The specimen was polished in the area of the slot.

A typical set of specimens is shown in figure III-3;² specimen prints are listed in table III-2 and are shown in figures III-4 through figure III-7. Specimen prints are dimensioned in conventional units only.

¹R. E. Peterson, "Stress Concentration Design Factors," John Wiley & Sons, Inc., New York, 1953.

²Some specimens shown have been tested and are failed.

Table III-2. Specimens Tested to Determine Effect of High-Pressure Gaseous Hydrogen Upon Mechanical Properties

Name	Print No.	Figure No.
Constant Strain Low-Cycle Fatigue Specimen	FML 95500B	III-4
Smooth Axial Fatigue Specimen (High-Cycle Fatigue)	FML 95212B	III-5
Fracture Mechanics Specimen	FML 95810	III-6
Flat End Creep-Rupture Specimen	FML 95623B	III-7
Ambient-Cryogenic Tensile Specimen (Notch)	FML 95620B	III-8
Ambient-Elevated Temperature Tensile Specimen (Smooth)	FML 95224B	III-9

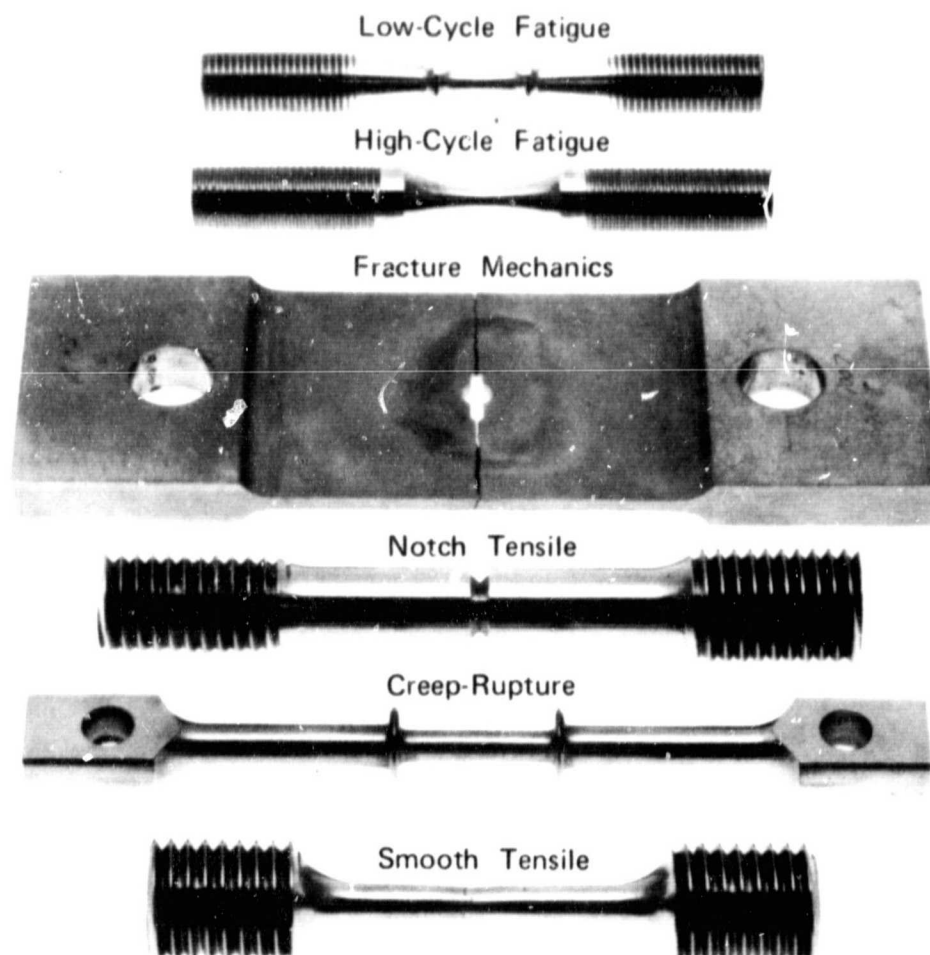
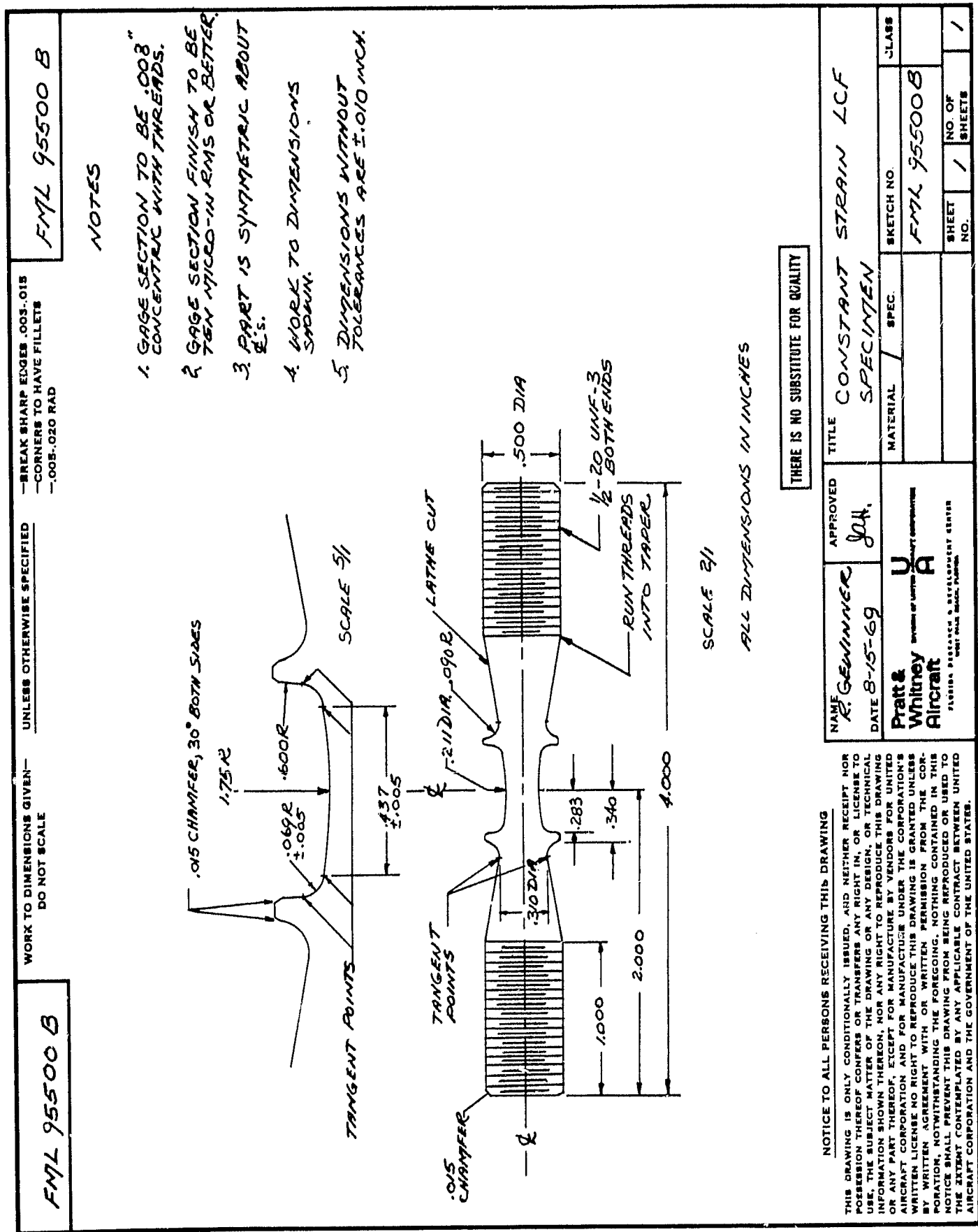


Figure III-3. Typical Test Specimens Used to Determine the Effect of High-Pressure Gaseous Hydrogen on Mechanical Properties of Materials

FE 119559A



FIL 95500B

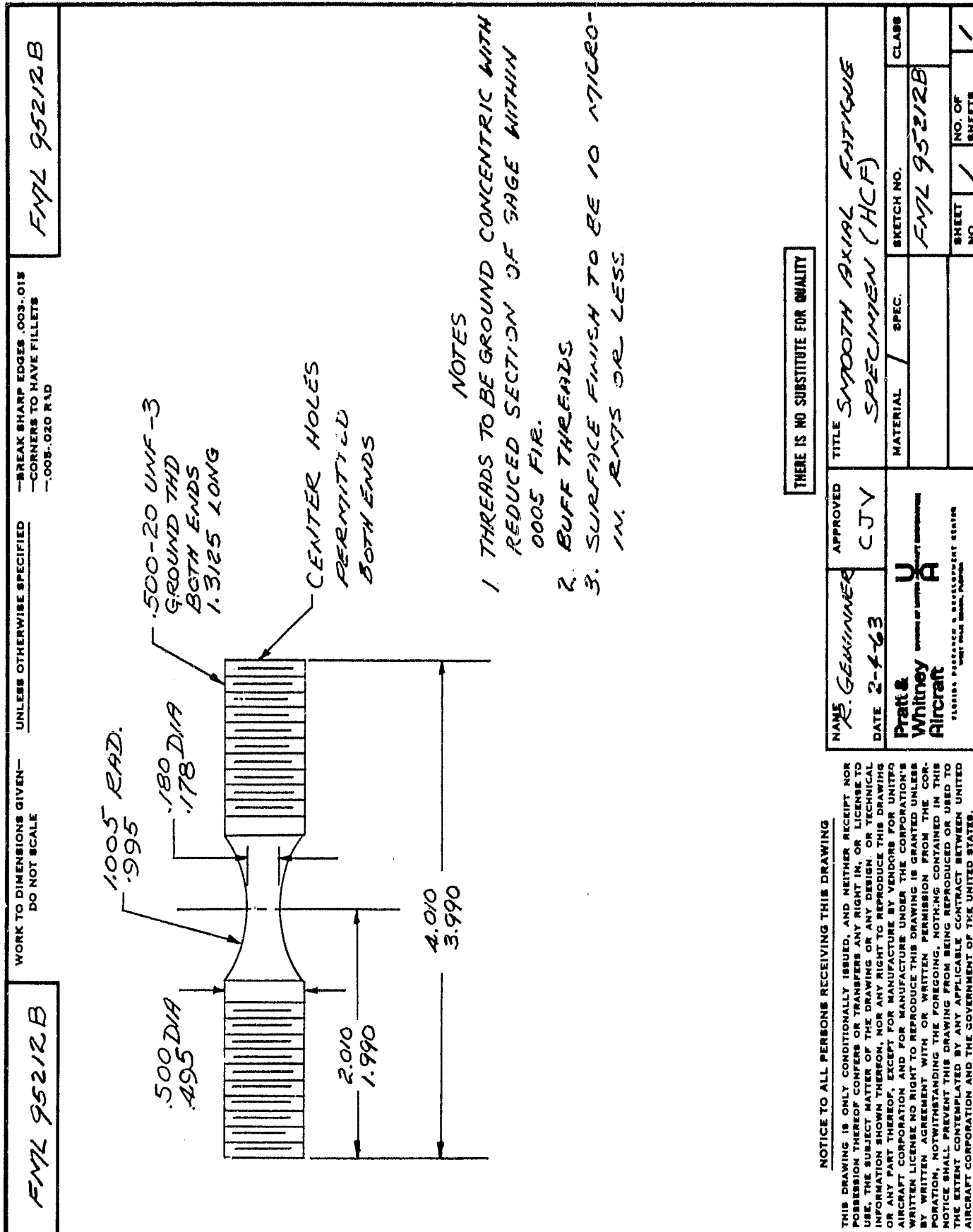
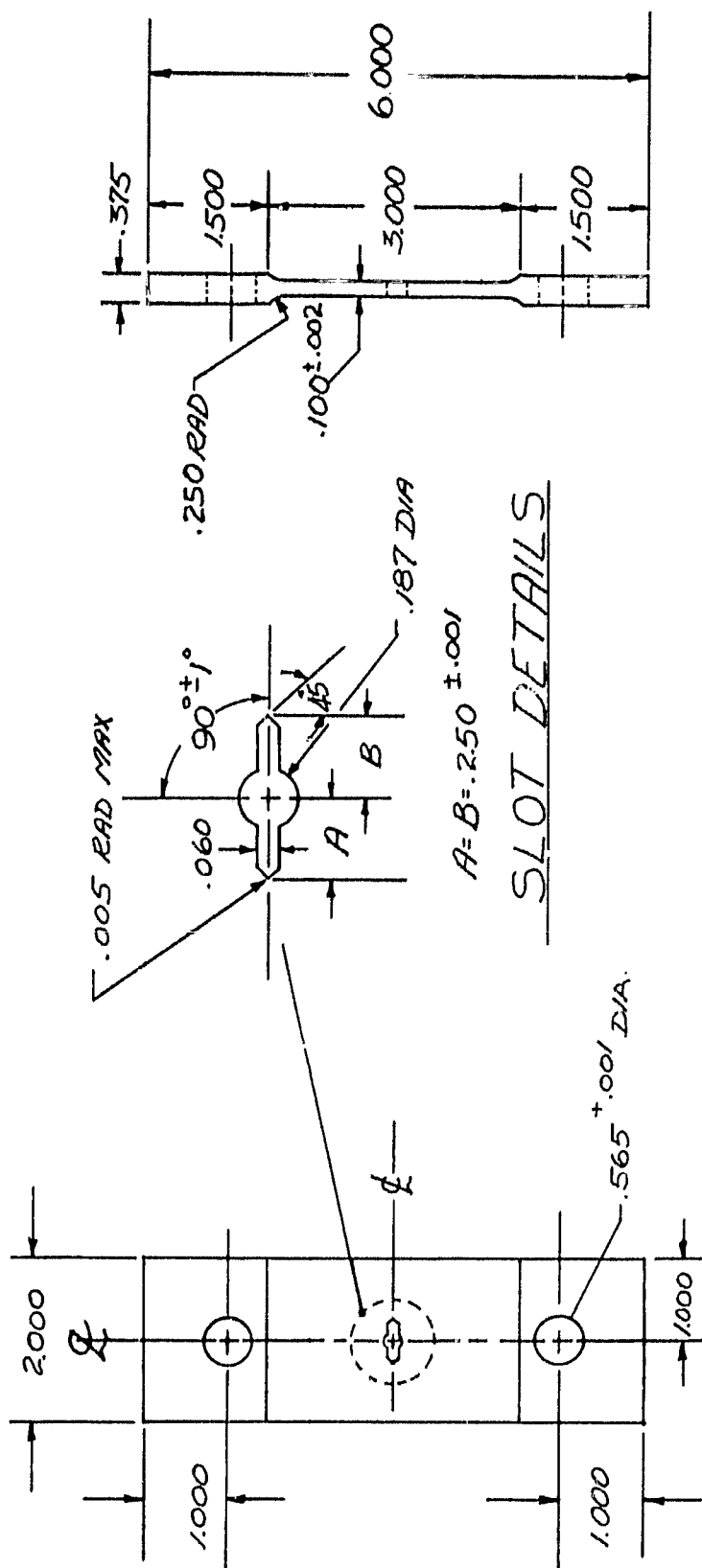


Figure III-5. Smooth Axial Fatigue Specimen (High-Cycle Fatigue)

01856 7443

—BREAK SHARP EDGES.003-.013
—CORNERS TO HAVE FILLETS
—.003-.025 RAD.

1. ALL DIM. $\pm .005$ U.O.S.
2. SLOT AND HOLES ON ϕ TO $\pm .001$.
3. GAGE SURFACES FLAT AND PARALLEL TO ± 0.002 T.I.R. WITH 10-16 U-IN. SURFACE FINISH.



ALTIMED NOJ EIMILISIOS OM SI JRESI

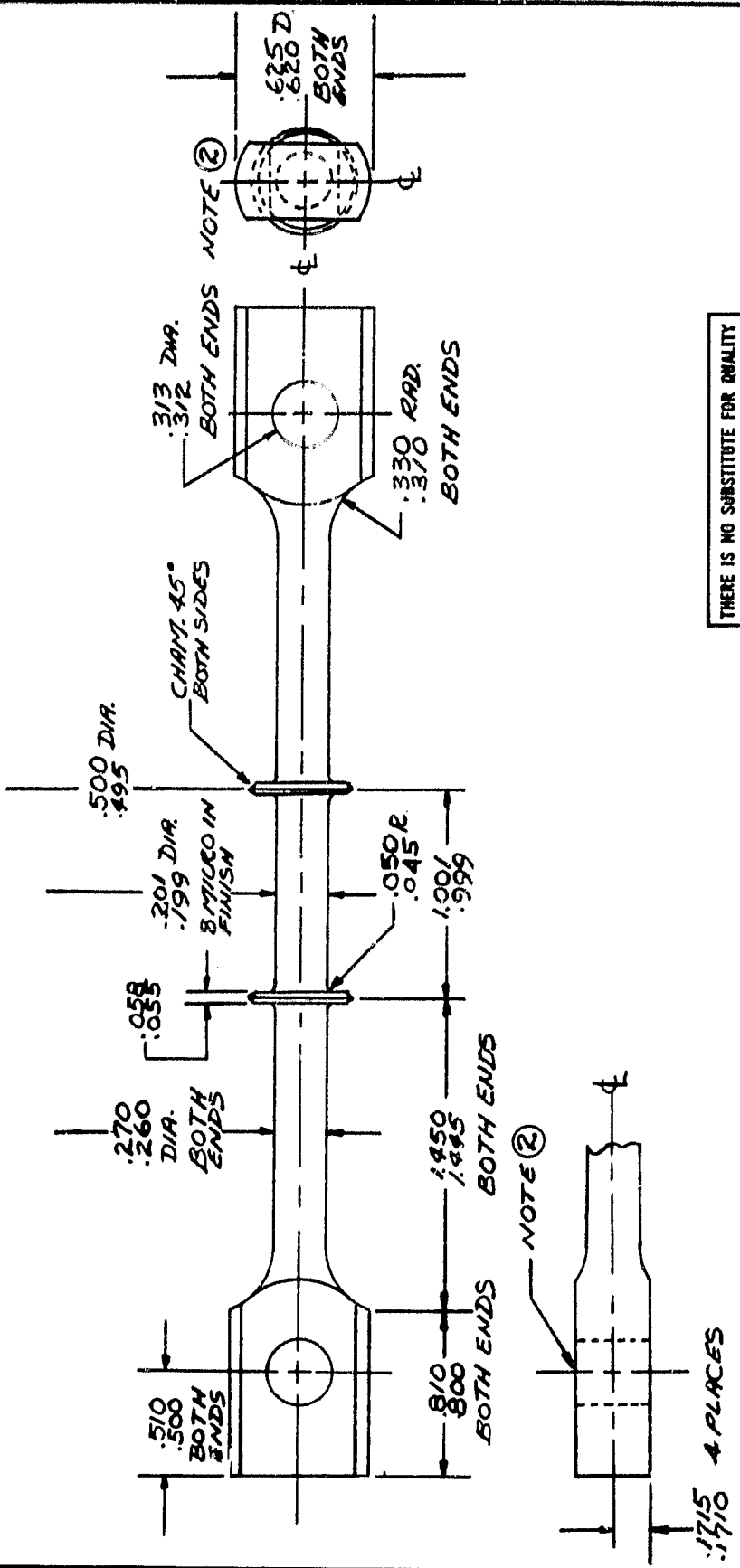
NOTICE TO ALL PERSONS RECEIVING THIS DRAWING

THIS DRAWING IS ONLY CONDITIONALLY ISSUED, AND NEITHER RECEIPT NOR POSSESSION THEREOF CONFERS OR TRANSFERS ANY RIGHT IN OR LICENSE TO REPRODUCE OR IN ANY MANNER DISCLOSE OR MAKE AVAILABLE TO ANY PERSON THE SUBJECT MATTER OF THE DRAWING OR ANY DESIGN OR TECHNICAL INFORMATION SHOWN THEREON, NOR ANY RIGHT TO REPRODUCE THIS DRAWING OR ANY PART THEREOF, EXCEPT FOR MANUFACTURE BY VENDORS FOR UNITED AIRCRAFT CORPORATION AND FOR MANUFACTURE UNDER THE CORPORATION'S WRITTEN LICENSE. NO RIGHT TO REPRODUCE THIS DRAWING IS GRANTED UNLESS BY WRITTEN AGREEMENT WITH OR WRITTEN PERMISSION FROM THE CORPORATION. NOTWITHSTANDING THE FOREGOING, NOTHING CONTAINED IN THIS NOTICE SHALL PREVENT THIS DRAWING FROM BEING REPRODUCED OR USED TO THE EXTENT SO COMTEMPLATED BY ANY APPLICABLE CONTRACT BETWEEN UNITED AIRCRAFT CORPORATION AND THE GOVERNMENT OF THE UNITED STATES.

NAME R. GEMINER DATE 10-29-71	APPROVED J. Harris	TITLE FRACTURE MECHANICS SPECIMEN			
Pratt & Whitney Aircraft DIVISION OF UNITED TECHNOLOGIES CORPORATION UTA FLORHAM PARK & DEVELOPMENT CENTER 1000 PARK DRIVE, PARSIPPANY, N.J. 07054		MATERIAL	SPEC.	SKETCH NO.	CLASS
				ENCL 95810	
		SHEET NO.	1	NO. OF PAGES	1

FML 95810

- ①-ALL DIAMETERS TO BE CONCENTRIC WITHIN $\pm .002$
- ②-HOLES TO BE PERPENDICULAR TO ϕ WITHIN $\pm .002$



NOTICE TO ALL PERSONS RECEIVING THIS DRAWING

THIS DRAWING IS ONLY CONDITIONALLY ISSUED, AND NEITHER RECEIPT NOR POSSESSION THEREOF CONFERS OR TRANSFERS ANY RIGHT IN, OR LICENSE TO USE, THE SUBJECT MATTER OF THE DRAWING OR ANY DESIGN, OR TECHNICAL INFORMATION SHOWN THEREON, NOR ANY RIGHT TO REPRODUCE THIS DRAWING OR ANY PART THEREOF, EXCEPT FOR MANUFACTURE BY VENDORS FOR UNITED AIRCRAFT CORPORATION AND FOR MANUFACTURE UNDER THE CORPORATION'S WRITTEN LICENSE NO RIGHT TO REPRODUCE THIS DRAWING IS GRANTED UNLESS BY WRITTEN AGREEMENT WITH OR WRITTEN PERMISSION FROM THE CORPORATION, NOTWITHSTANDING THE FOREGOING, NOTHING CONTAINED IN THIS NOTICE SHALL PREVENT THIS DRAWING FROM BEING REPRODUCED OR USED TO THE EXTENT CONTEMPLATED BY ANY APPLICABLE CONTRACT BETWEEN UNITED AIRCRAFT CORPORATION AND THE GOVERNMENT OF THE UNITED STATES.

PWA - 10000 - REV - 5-83

NAME R. GENWINGER	APPROVED J.S.	TITLE FLAT END CREEP RUPTURE SPECIMEN
DATE Jan '70	MATERIAL SPEC.	CLASS
Pratt & Whitney Aircraft FLEET RESEARCH & DEVELOPMENT CENTER WEST PALM BEACH, FLORIDA	SKETCH NO. FML 95623 B	NO. OF SHEETS

Figure III-7. Flat End Creep-Rupture Specimen

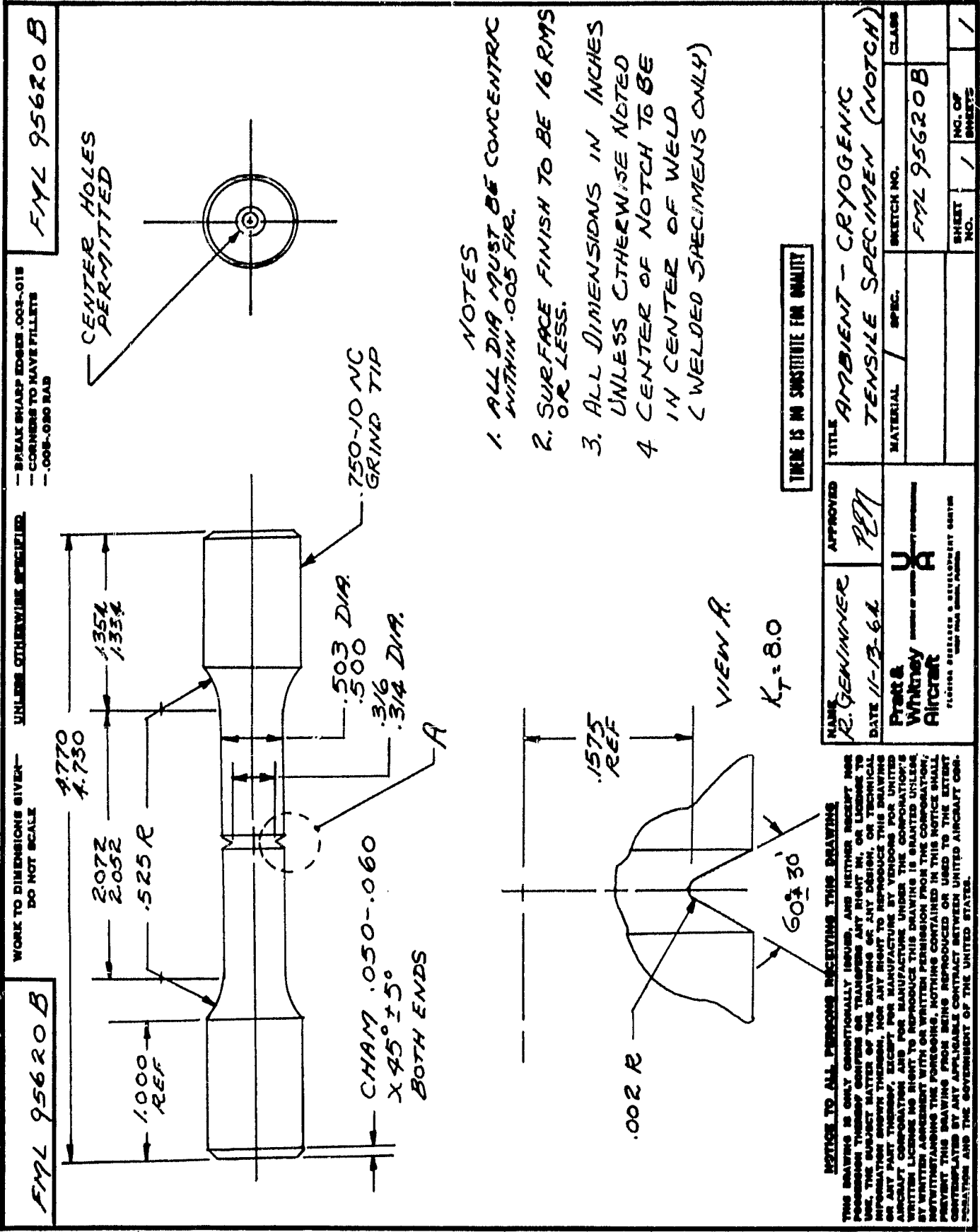


Figure III-8. Ambient-Cryogenic Tensile Specimen (Notch)

FWL 95620B



SECTION IV LOW-CYCLE FATIGUE

Low-cycle fatigue (LCF) tests were conducted at 34.5-MN/m^2 (5000-psig) pressure and 951°K (1250°F) to determine the gaseous hydrogen degradation of one cast nickel-base, one wrought nickel-base, and one wrought cobalt-base alloy. Comparison of axial constant strain tests in a high-pressure hydrogen environment with results of similar tests in a helium environment establishes degradation due to the hydrogen environment. The low-cycle fatigue tests have been of the strain-controlled type with the material cycling through a constant, all tensile, total (elastic plus plastic) strain range (figure IV-1) until complete specimen fracture.

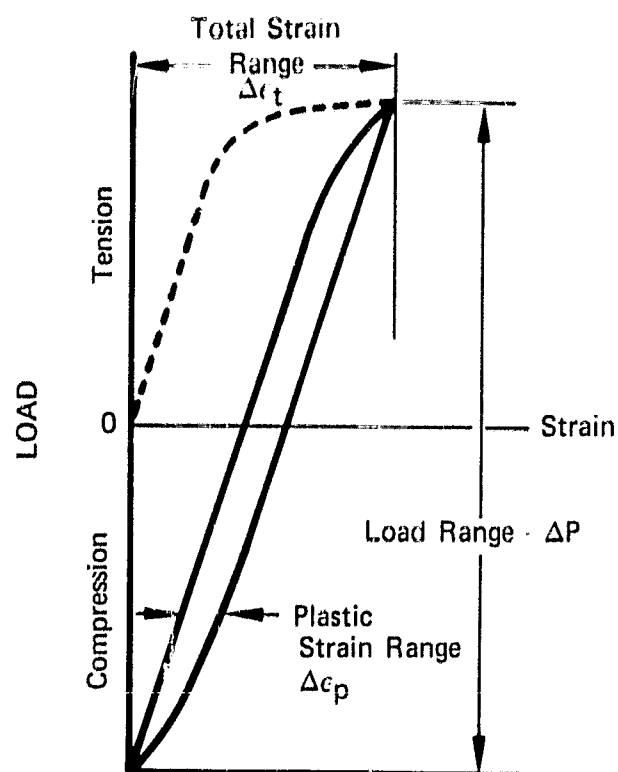


Figure IV-1. Typical Load-Strain Hysteresis Curve
Obtained During a Specimen LCF Test

FD 48672

A. CONCLUSIONS AND DISCUSSION

All materials tested had indications of degradation in LCF life due to high-pressure hydrogen. The most severely degraded alloy was IN100, followed by Haynes 188 and WASPALOY®. Due to the limited number of tests conducted in helium, conclusions pertaining to the degree of degradation must be general in nature. Comparisons of degradation at given total strain ranges have to be based upon extrapolation of data, and extrapolation of data curves could introduce unacceptable errors. However, there is a trend for a decreasing degree of degradation with decreasing total strain range, indicating strain (total and plastic) level sensitivity. All LCF testing was conducted at 951°K (1250°F); therefore, no conclusions regarding degradation versus temperature could be made. Complete test results are listed in table IV-1 and plotted in figures IV-2 through IV-4.

Table IV-1. Elevated Temperature, Low-Cycle Fatigue Properties in High-Pressure Gaseous Environment

Material	Test Temperature, °K °F		Test Conditions			Total Strain Range, %	Test Results		
			Environ-ment	MN/m ²	Pressure, psi		Cyclic Rate, Cycles/min	Cycles to Failure	Plastic Strain Range*, %
IN100	951	1250	Helium	34.5	5000	1.00	4	630	<0.05
	951	1250	Helium	34.5	5000	0.80	4	1,820	<0.05
	951	1250	Hydrogen	34.5	5000	1.00	4	190	<0.05
	951	1250	Hydrogen	34.5	5000	0.90	4	315	<0.05
	951	1250	Hydrogen	34.5	5000	0.80	5	650	<0.05
	951	1250	Hydrogen	34.5	5000	0.60	5	1,450	<0.05
Haynes 188	951	1250	Helium	34.5	5000	1.80	3	1,050	0.88 - 1.00
	951	1250	Helium	34.5	5000	1.25	4	1,151	0.33 - 0.65
	951	1250	Helium	34.5	5000	1.45	3	765	0.79 - 1.09
	951	1250	Hydrogen	34.5	5000	1.45	3	470	0.71 - 0.95
	951	1250	Hydrogen	34.5	5000	1.30	4	720	0.50 - 0.84
	951	1250	Hydrogen	34.5	5000	1.15	4	1,106	0.22 - 0.41
WASPALLOY®	951	1250	Hydrogen	34.5	5000	1.10	4	1,423	0.31 - 0.53
	951	1250	Helium	34.5	5000	1.80	3	202	0.34 - 0.36
	951	1250	Helium	34.5	5000	1.20	4	980	0.14 - 0.17
	951	1250	Hydrogen	34.5	5000	1.80	3	105	0.45 - 0.50
	951	1250	Hydrogen	34.5	5000	1.50	3	260	0.24 - 0.30
	951	1250	Hydrogen	34.5	5000	1.30	4	600	0.16 - 0.20
	951	1250	Hydrogen	34.5	5000	1.00	4	1,950	0.10 - 0.13

*Includes strain hardening - softening effects.

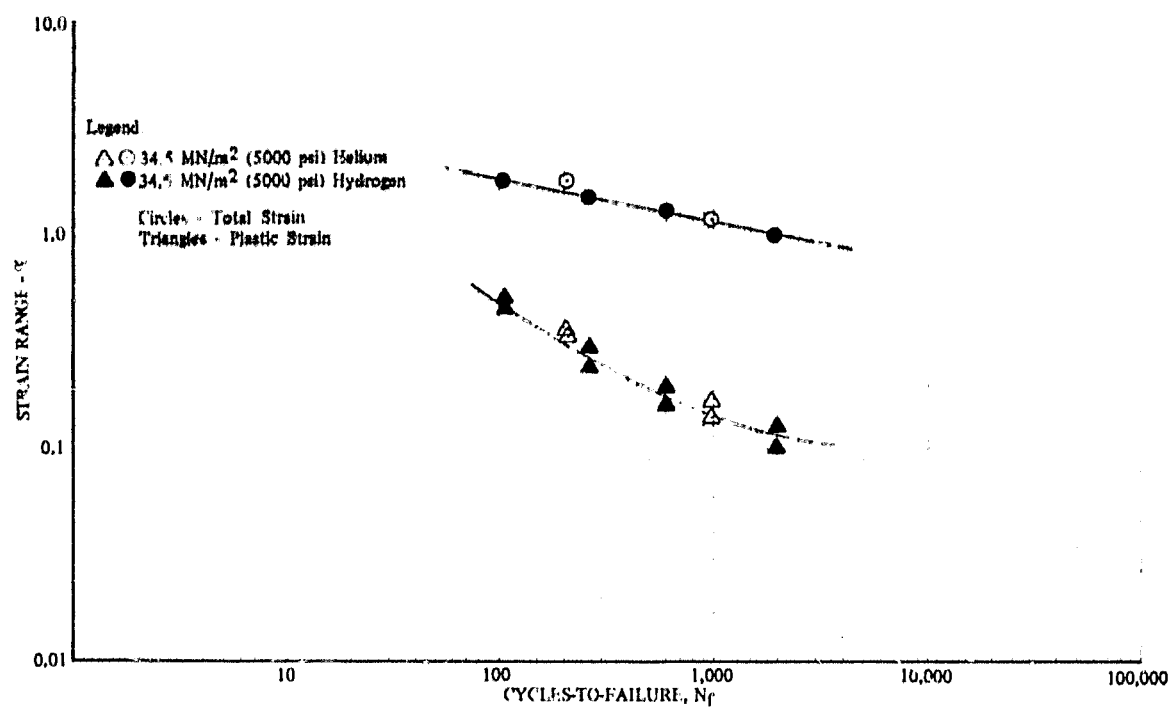


Figure IV-2. Low-Cycle Fatigue Life of Waspaloy[®] DF 91283
at 951°K (1250°F)

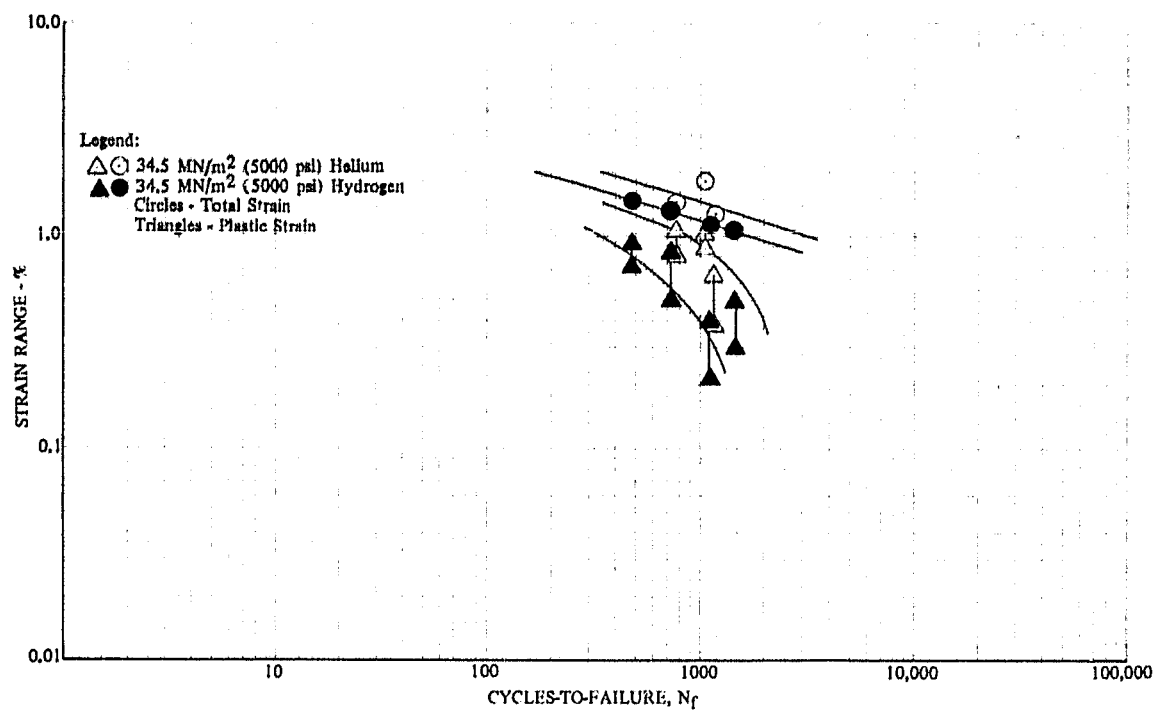


Figure IV-3. Low-Cycle Fatigue Life of Haynes 188 DF 91284
at 951°K (1250°F)

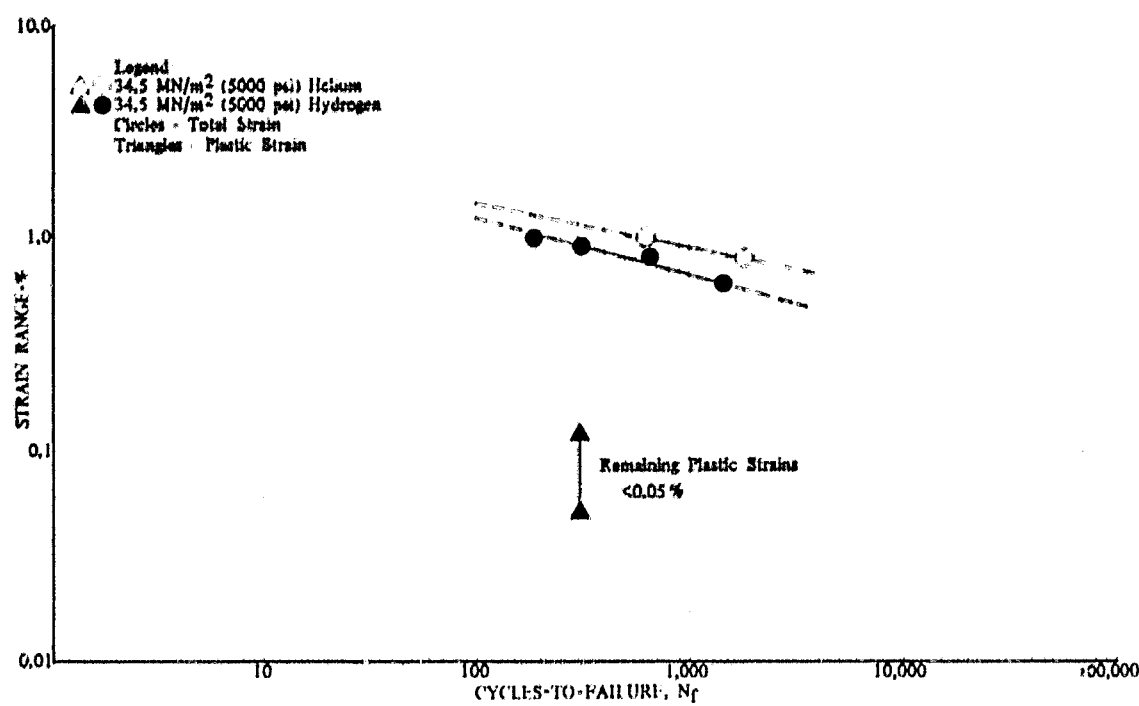


Figure IV-4. Low-Cycle Fatigue Life of IN100 at 951°K (1250°F) DF 91285

B. TEST PROCEDURES

Smooth, round, solid specimens were used for the strain-controlled LCF tests discussed in this report. The test specimen used is described in Section III and detailed in figure III-4. The specimen configuration incorporates integral machined extensometer collars. A calibration procedure was established for each material to relate the maximum strain to collar deflection during both the elastic and plastic portion of the strain cycle. The specimen design and calibration procedure were verified both experimentally and analytically.

After machining, specimen gage sections were polished and dimensions measured. Prior to installation in the test rig, specimens were thoroughly cleaned with a nonchlorinated solvent.

Tests were conducted on a closed-loop-type, hydraulically actuated test machine, which was designed and built by P&WA, and located in an isolated test cell. Specimen axial strain is measured and controlled by means of a proximity probe extensometer. A heavy walled pressure vessel made of AISI type 347 stainless steel, described in PWA FR-4566, was used. This vessel incorporates a GrayLocc-type flange and seal and includes a pressure compensating device to eliminate the axial tensile load acting over the differential specimen and adapter areas. During testing, load-strain hysteresis curves are plotted using the extensometer and internal load cell outputs. Electrical connections to the load cell, extensometer system, furnace (for elevated temperature tests only), and thermocouples are made through the vessel wall via high-pressure bulkhead connectors.

Elevated temperatures are obtained with a resistance furnace surrounding the specimen internal to the pressure vessel. A dc power supply and controller were used to drive the furnace. Thermocouples attached to the specimen are used to monitor and control temperature during test. Because of the short specimen

gage section, a single-zone furnace was adequate to maintain a uniform gage section temperature. The high thermal conductivities of high-pressure helium and hydrogen gases enable the load cell and strain measuring transducer of the extensometer to operate at safe temperatures because of their location in the bottom of the vessel.

After inserting the prepared specimen in the test vessel and attaching the extensometer, the vessel was sealed and subjected to a purge cycle consisting of a nitrogen purge, evacuation, test gas (helium or hydrogen) purge, and, finally, a pressurized pop purge. The pop purge consists of rapidly pressurizing the vessel to a low pressure (typically 250 psig) with test gas and releasing several times, while maintaining a minimum positive gas pressure.

After purging, high-pressure gas is introduced and maintained in the vessel until specimen temperature and gas pressure are stabilized at the desired level and testing conducted. The test machine control provides automatic system shutdown upon specimen fracture. Test gas is then vented (and vessel purged with nitrogen in the case of hydrogen tests), the vessel opened, and the specimen removed.

SECTION V HIGH-CYCLE FATIGUE

A. INTRODUCTION

Tests were accomplished on two nickel-base alloys (MAR M-200 DS and IN100) to evaluate the high-cycle fatigue (HCF) behavior of these materials when subjected to high-pressure gaseous helium and hydrogen atmospheres at elevated temperature and to establish the susceptibility of these alloys to hydrogen degradation.

High-cycle fatigue (HCF) tests were conducted in 34.5-MN/m² (5000-psig) gaseous helium and hydrogen at 951°K (1250°F) for both materials investigated. Results of the helium tests provided a baseline for comparison with the hydrogen tests.

B. CONCLUSIONS AND DISCUSSION

Tests of the MAR M-200 DS alloy at 951°K (1250°F) in 34.5-MN/m² (5000-psig) hydrogen indicated an appreciable HCF life degradation (figure V-1). All specimens tested in helium atmosphere were examined metallurgically subsequent to failure to determine possible explanation of data scatter. All specimens examined showed numerous small fractures along the gage section and numerous cracks through MC carbides and some incipient melting from the 1477°K (2200°F) solution cycle. However, all specimens examined showed satisfactory grain orientation with some, but not excessive, micro shrinkage evident (figure V-2). The slope of the helium HCF baseline S-N curve was established by the half-cycle ultimate tensile strength (1208.7 MN/m², [175.3 ksi]) at 951°K (1250°F) in helium and the cycles-to-failure for a HCF specimen at the average maximum stress level (1068.7 MN/m² [155 ksi]) tested. Due to the low cycles-to-failure established for baseline test, hydrogen test maximum stress levels were selected to yield test data within the same cycle range for a more comprehensive analysis.

The HCF life of the IN100 alloy at 951°K (1250°F) was slightly degraded (approximately 37.9 MN/m² [5.5 ksi] at 10⁴ cycles) by the 34.5-MN/m² (5000-psig) hydrogen environment (figure V-3). Specimens tested in both helium and hydrogen were examined metallurgically subsequent to test and one specimen tested in hydrogen atmosphere (figures V-3 and V-4) exhibited excessive micro shrinkage.

C. TEST PROCEDURE

Smooth, round specimens were used for the high-cycle fatigue tests discussed in this report. The test specimen is illustrated in Section III and is detailed in figure III-5.

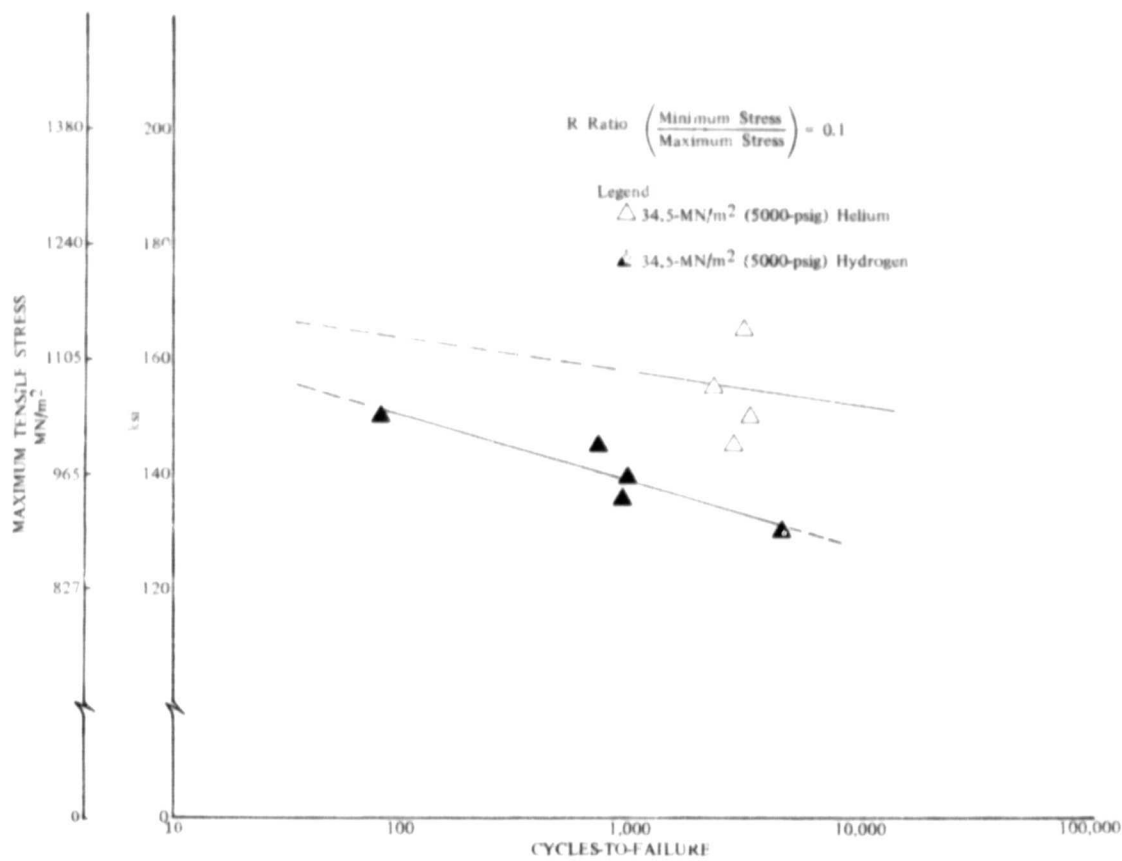


Figure V-1. High-Cycle Fatigue Life of MAR M-200 DS at 1250° F DF 91088

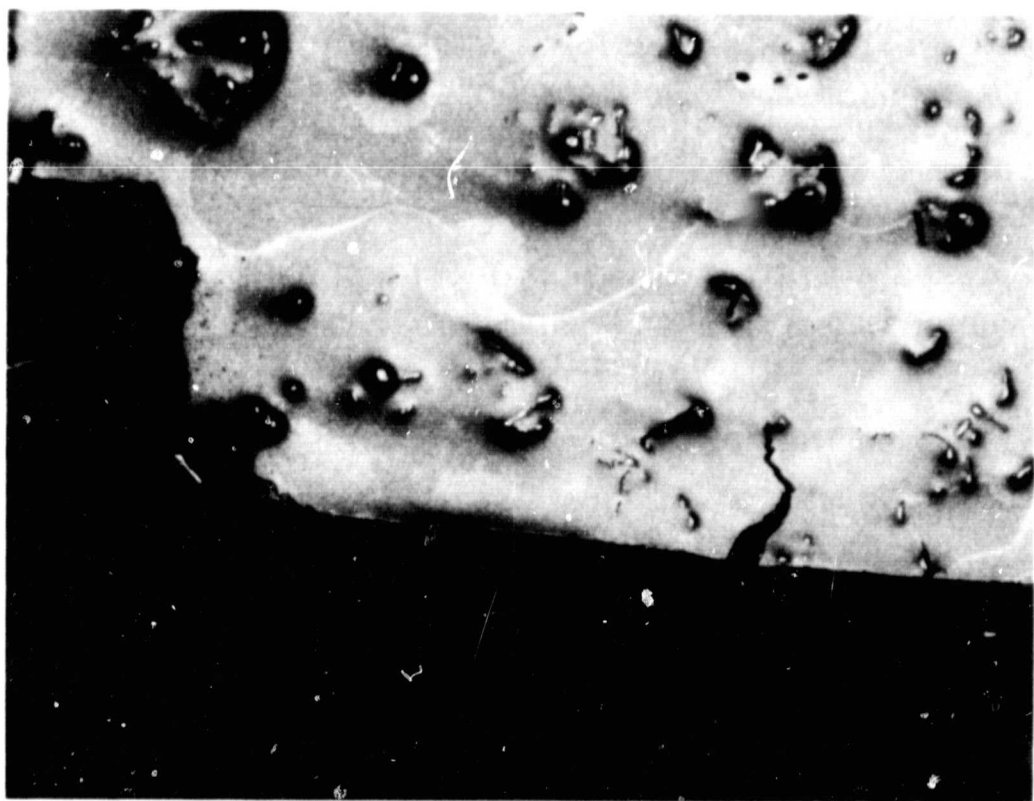


Figure V-2. Typical MAR M-200 DS Cross Section Adjacent to Fracture Face (Mag: 100X) FAM 76146

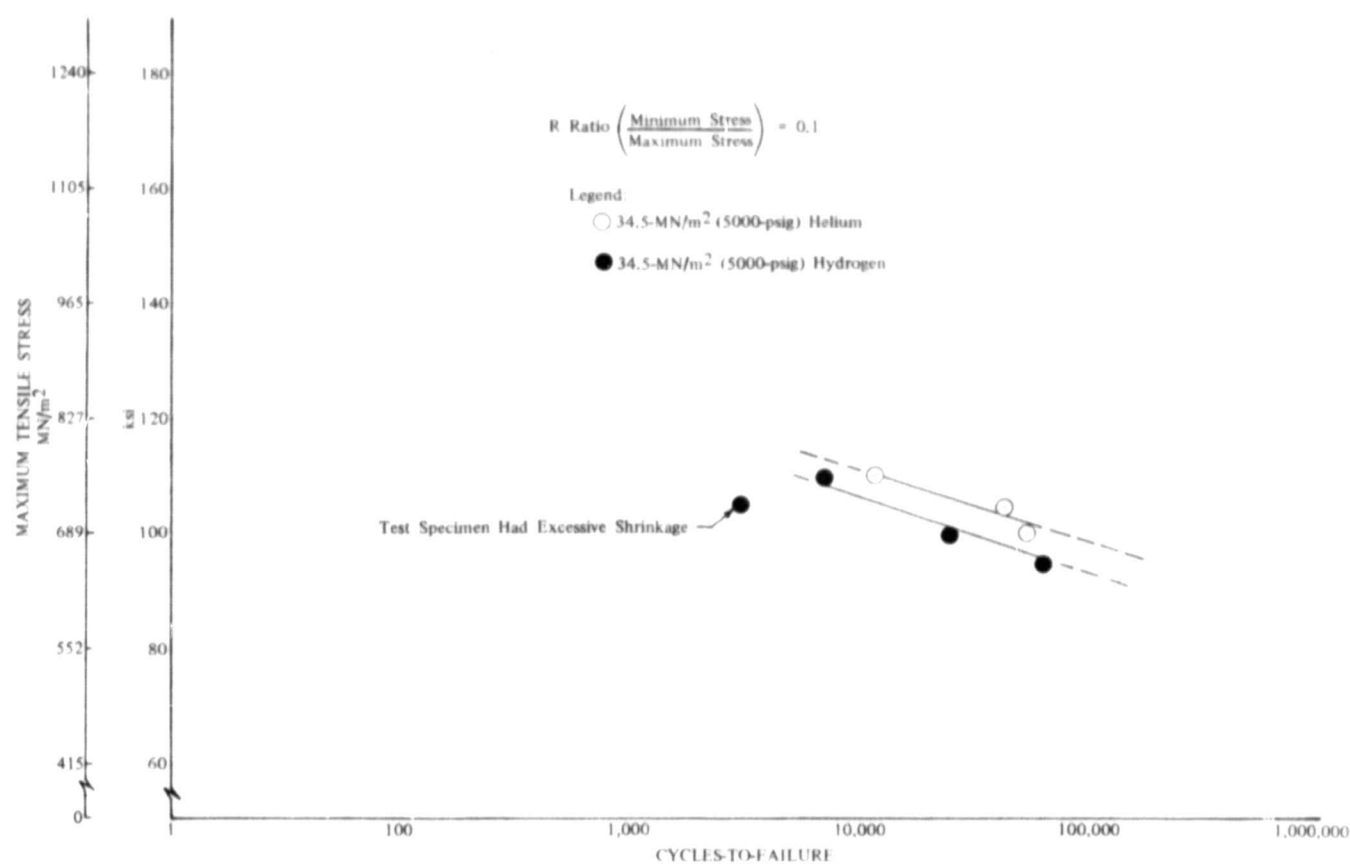


Figure V-3. High-Cycle Fatigue Life of IN100 at 1250° F DF 91089

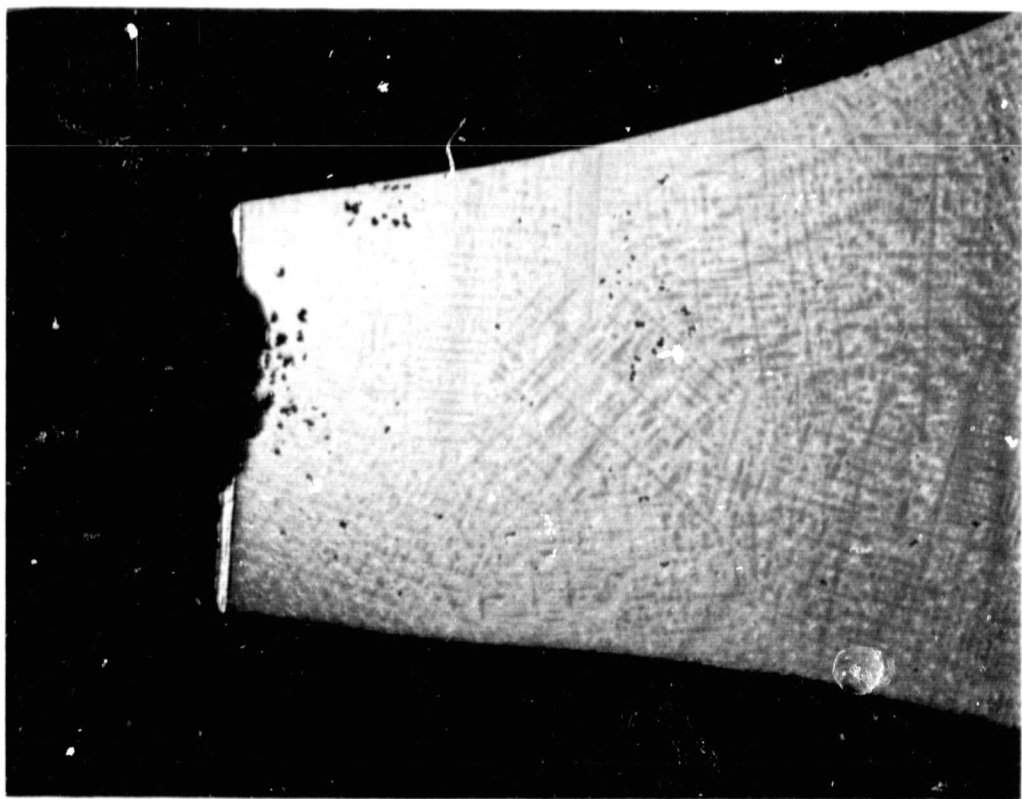


Figure V-4. Macrograph of IN100 Test Specimen Showing Excessive Micro Shrinkage at Fracture Face (Mag: 10X) FAL 25016

Pratt & Whitney Aircraft

PWA FR-5129

Subsequent to machining, specimen material was verified, each specimen was inspected visually for any machining discrepancies and X-ray inspected to detect any internal flaws. Prior to testing, each specimen gage section (minimum cross section) was measured to the nearest 0.0005 in. (0.012 mm) with a micrometer and cleaned with acetone.

The HCF life data were established by an axial load (stress) controlled tension-tension test. A typical test cycle is a tensile load that varies sinusoidally about a constant tensile preload at a cyclic rate of 20 Hz. All specimens were tested at an R ratio (minimum stress/maximum stress) of 0.1.

Tests were conducted using a closed-loop, servocontrolled, hydraulically actuated test machine located in an isolated test cell. The test specimen was mounted in a heavy walled pressure vessel attached to the upper platen of the test machine. Test specimens were mounted in the pressure vessel load frame by threading each end into tapped loading rods (top and bottom) and securing each end with locknuts. The specimen and the sealed pressure vessel were subjected to a purge cycle, consisting of nitrogen purge, evacuation, two successive pop purges with the test media (helium or hydrogen), and final pressurization to test pressure.

Specimen load was measured by a strain gage-type load cell, integral with the specimen loading rod and inside the pressure vessel. Prior to the initial test and periodically throughout the test program, the load cell calibration was checked (using an instrumented and calibrated specimen) at 34.5-MN/m² (5000-psig) pressure, so that axial tensile loads on the specimen due to high pressure acting over differential specimen and loading rod areas could be compensated for by the loading system. Since the load cell was adjacent to and calibrated to give absolute specimen load, friction loss through the loading rod O-ring seals is of no consequence. Electrical connections to all internal strain gages, load cell, thermocouples, and heating devices were made through the bottom of the pressure vessel via an instrumentation manifold and high-pressure bulkhead connectors. During testing, the load cycle and number of cycles-to-failure were constantly monitored on a calibrated oscilloscope and electronic counter using the internal load cell output.

Elevated temperature testing was accomplished using a dc power supply and high-power-density, single-zone furnace mounted inside the pressure vessel and around the test specimen. Analysis of gas samples, before and after the specimen tests, indicated required maximum oxygen levels were met during testing. Thermocouples looped around the specimen minimum cross section were used to monitor and control specimen temperature during each test.

Test system shutdown was provided at the instant of specimen failure by a linear variable differential transformer, which sensed load rod position in combination with a meter relay. This proved an accurate method of determining the total number of cycles-to-failure.

D. RESULTS

Maximum stress level and cycles-to-failure data were obtained for each test material and are listed in table V-1. These data are presented graphically (figures V-1 and V-3) to obtain stress vs cycles-to-failure (S-N) curves for each material. The difference in the HCF curves for the helium and hydrogen tests represent the degradation of high-cycle fatigue life of each material tested as a result of high-pressure hydrogen at 951°K (1250° F).

Table V-1. Elevated-Temperature, High-Cycle Fatigue Properties of Materials in High-Pressure Gaseous Environments

Material	Test Temperature,		Environment	Test Conditions				Cyclic Rate, Hz	Cycles-to-Failure
	°K	°F		Pressure, MN/m ²	Test Pressure, psi	Stress* Level Maximum, MN/m ²	ksi		
IN100	951	1250	Helium	34.5	5000	689.48	100.0	20	50,600
	951	1250	Helium	34.5	5000	723.95	105.0	20	43,000
	951	1250	Helium	34.5	5000	758.42	110.0	20	11,100
	951	1250	Hydrogen	34.5	5000	655.00	95.0	20	60,700
	951	1250	Hydrogen	34.5	5000	689.48	100	20	24,400
	951	1250	Hydrogen	34.5	5000	723.95	105	20	2,860
	951	1250	Hydrogen	34.5	5000	758.42	110	20	6,900
MAR M-200 DS	951	1250	Helium	34.5	5000	999.74	145	20	2,630
	951	1250	Helium	34.5	5000	1034.22	150	20	3,100
	951	1250	Helium	34.5	5000	1069.00	155	20	2,200
	951	1250	Helium	34.5	5000	1138.63	165	20	2,800
	951	1250	Hydrogen	34.5	5000	896.32	130	20	4,265
	951	1250	Hydrogen	34.5	5000	930.00	135	20	890
	951	1250	Hydrogen	34.5	5000	965.26	140	20	935
	951	1250	Hydrogen	34.5	5000	999.74	145	20	680
	951	1250	Hydrogen	34.5	5000	1034.22	150	20	80
*Stress levels for R ratio									
$\frac{\text{Minimum Stress}}{\text{Maximum Stress}} = 0.1$									

SECTION VI FRACTURE MECHANICS TESTING

A. INTRODUCTION

Fracture mechanics tests, consisting of fracture toughness, and cyclic and sustained-load, were conducted using preflawed center-cracked specimens in 34.5-MN/m² (5000-psig) gaseous hydrogen at a temperature of 300°K (80°F). For comparison, one fracture toughness test was conducted in 34.5-MN/m² (5000-psig) pressure helium. The material tested (Section III) was AMS 5706 WASPALOY[®], fully heat treated.

B. RESULTS AND CONCLUSIONS

The following conclusions were made from the results of the fracture mechanics testing program and investigations relating thereto:

1. Significantly lower fracture toughness values for AMS 5706 WASPALOY occurred at 300°K (80°F) in 34.5-MN/m² (5000-psig) hydrogen as compared to helium. Fracture toughness values of 63 to 74 MN/m² √m (57 to 67 ksi√in.) occurred in hydrogen as compared to 103 MN/m² √m (93 ksi√in.) in helium.
2. Cyclic flaw growth data and sustained load flaw growth data are presented in graphical form in figures VI-1 and VI-2, respectively. An initial stress intensity value of approximately 27.9 MN/m² (25 ksi√in.) would be required for 100 cycle life in 34.5-MN/m² (5000-psig) hydrogen at 300°K (80°F). This is a ratio of initial stress intensity to critical stress intensity of approximately 0.45.
3. A sustained-load threshold stress intensity K_{TH} of approximately 33 MN/m² √m (30 ksi√in.) would yield no flaw growth at 100 hr at 300°K (80°F) and 34.5-MN/m² (5000-psig) hydrogen pressure.

C. TEST PROCEDURE

Specimen blanks were cut from rectangular bar stock, heat treated, and machined into center-cracked specimens per figure III-6. All specimens were machined to a thickness of 2.45 mm (0.100 in.) in the gage section. This thickness was selected to stay within the load limits of the existing high-pressure test equipment. All specimens were precracked in tension-tension using a Sonntag fatigue machine, which operates at 30 Hz (1800 cpm). Precracking was conducted in air at approximately 300°K (80°F) at load levels (K_f), which later were verified, not to exceed 60% of K_Q.

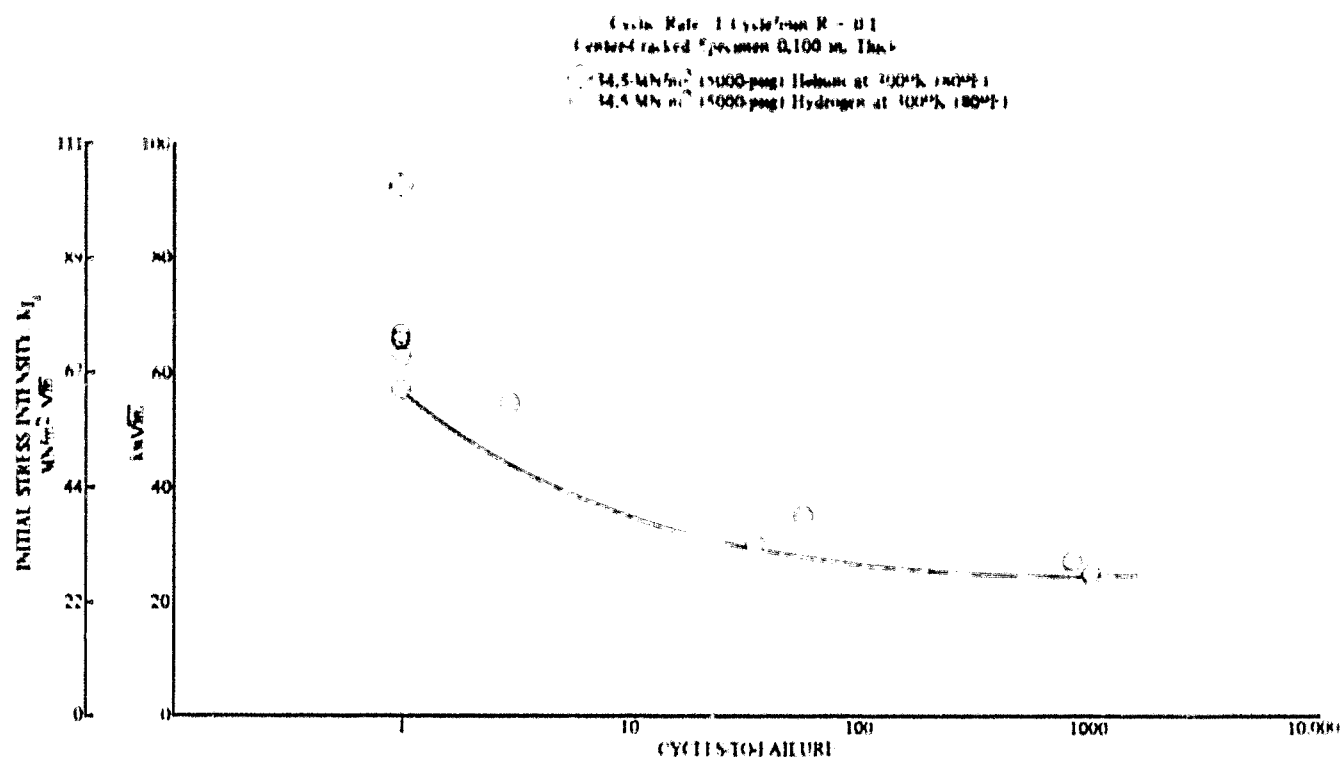


Figure VI-1. Cyclic Flaw Growth Data for AMS 5706 WASPALOY® DF 91090

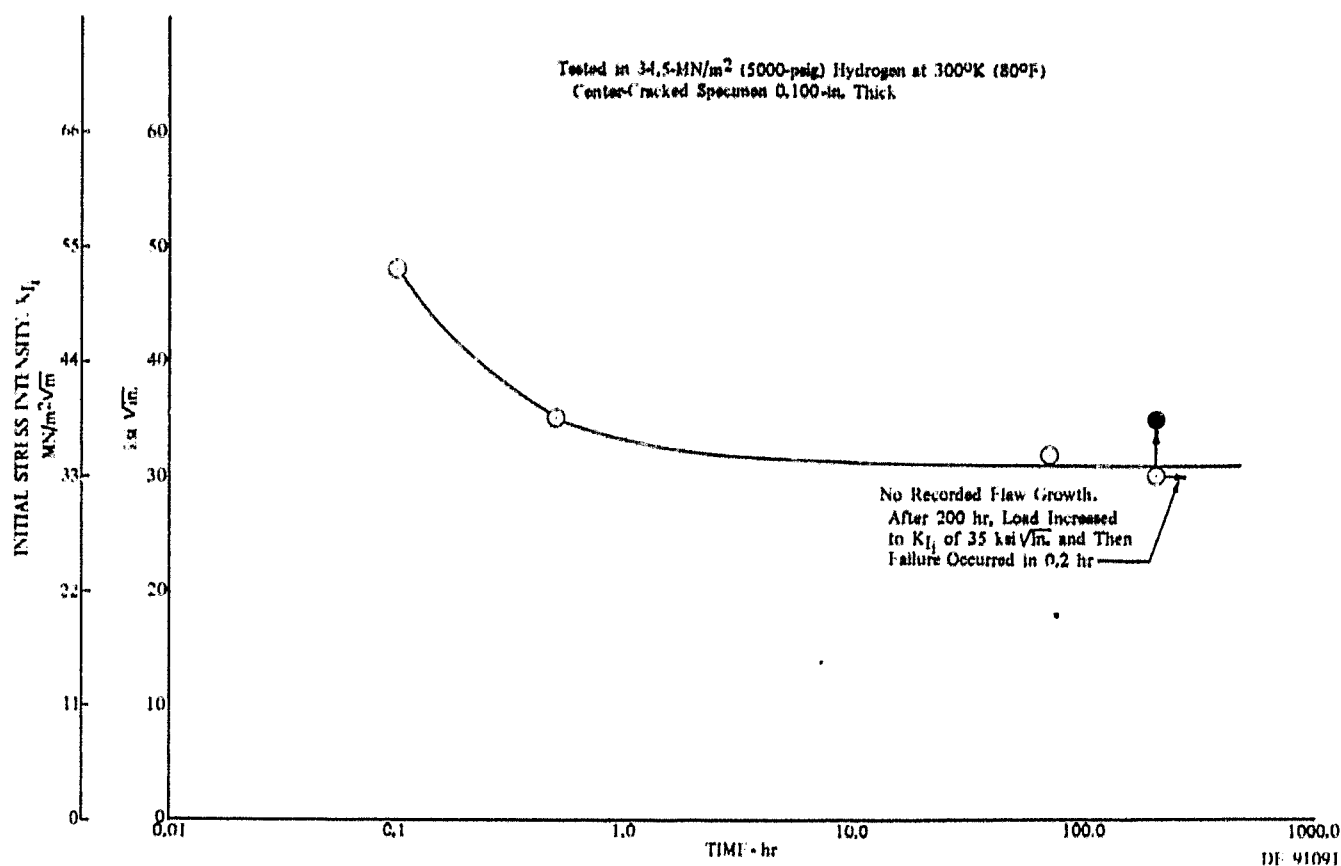


Figure VI-2. Sustained-Load Flaw Growth Data for AMS 5706 WASPALOY® DF 91091

1. Equipment

Fracture toughness testing was conducted on a 133.4 kN (30,000-lb) Tinius Olsen testing machine. This equipment is shown in figures VI-3 and VI-4. An internal load cell is used, thus the effects of friction on the load rod are not recorded on the readout equipment. To make the necessary gas analyses, a gas sampling system is incorporated in the test cell.

Fracture Mechanics testing was conducted on a P&WA-designed and built, hydraulically actuated test machine.

Dead-weight loading was attained by replacing hydraulic actuation with actuation of a ram by a large reservoir of 11.6-MN/m² (1700-psig) nitrogen. The heavy walled pressure vessel was mounted on the upper platen of the test machine. The base of the vessel includes a pressure-compensating device to eliminate the axial tensile load acting over the differential specimen and adapter areas. Both internal (to the pressure vessel) and external load cells are used, thus the effect of friction at the seals, where the load rods enter the vessel, is considered.

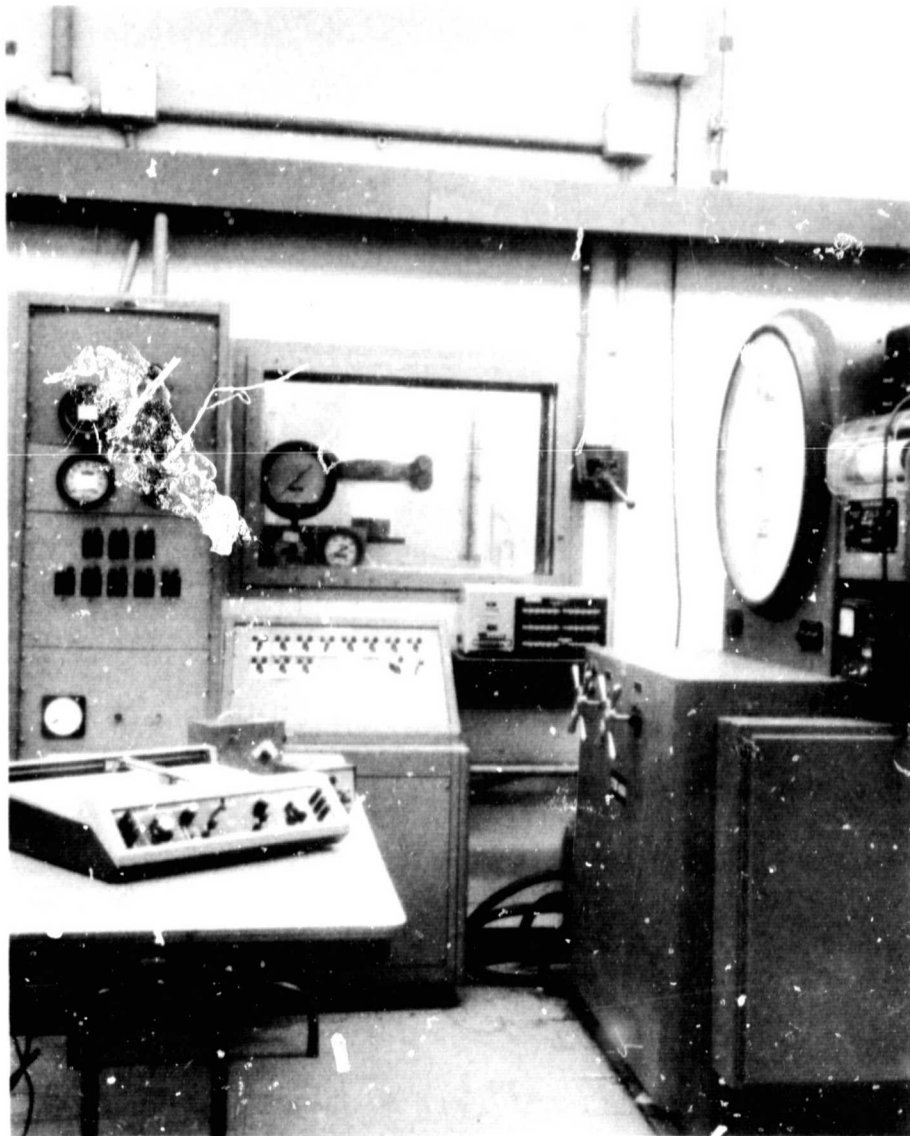


Figure VI-3. Tensile Machine, Test Environment
Controls, and Data Acquisition
Equipment Located in the Blockhouse

FC 21272

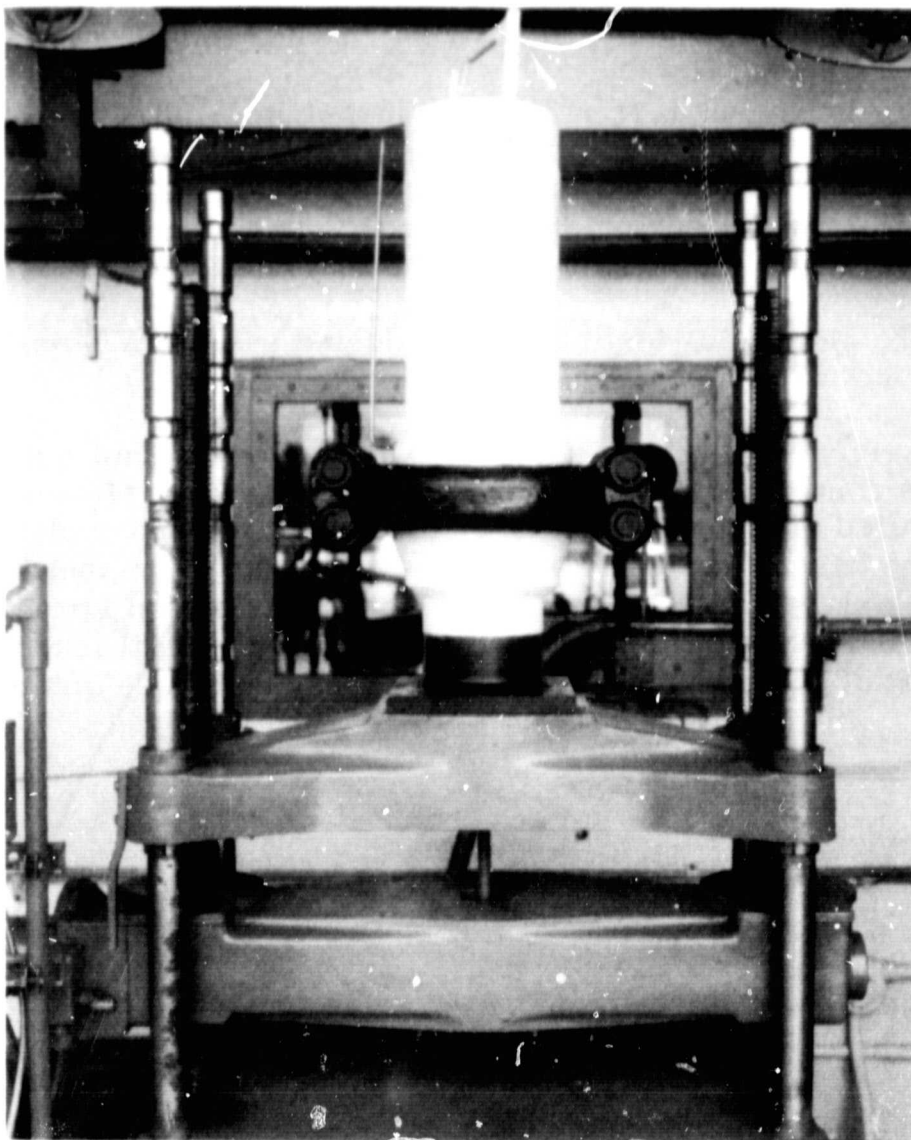


Figure VI-4. High-Pressure Gaseous Environment
Fracture Toughness Test Vessel
Installed on Tensile Machine in the
Test Cell

FC 21268

2. Test Method

The following procedure is used during testing:

- a. Specimen is precracked per ASTM Designation E 399-70T.
- b. Fracture toughness values and initial stress intensities were calculated using the Brown and Srawley equation, as reported in ASTM STP 410 for center-cracked, finite-width specimens. The equation is as follows:

$$K_I = \frac{P a^{1/2}}{BW} [1.77 + 0.277 (2a/w) - 0.510 (2a/w)^2 + 2.7 (2a/w)^3]$$

Where:

P = load, N (lb)

B = thickness, mm (in.)

W = width, mm (in.)

$2a$ = total crack length, mm (in.)

K_I = stress intensity, $\text{MN}/\text{m}^2 \sqrt{\text{m}}$ (ksi $\sqrt{\text{in.}}$)

The bracketed series expansion is the finite width correction factor.

- c. Chamber is opened and prepared specimen installed and instrumentation continuity checks conducted.
- d. Chamber is closed, sealed, and evacuated, then backfilled and purged four times in succession with the test gas.
- e. Chamber is pressurized with test gas to $34.5 \text{ MN}/\text{m}^2$ (5000-psig)
- f. Test is conducted. During testing the load-time curve is plotted on an x-y recorder from the output of the internal load cell. Crack propagation with time was monitored during K_{TH} testing by following the crack front with crack propagation continuity gages.
- g. Following specimen failure, the chamber is vented, and the failed specimen is removed.
- h. Test results are analyzed from the recorded test data.

SECTION VII
CREEP RUPTURE

A. INTRODUCTION

Creep-rupture properties were evaluated under 34.5-MN/m² (5000-psig) hydrogen, 34.5-MN/m² (5000-psig) hydrogen/water vapor, and 34.5-MN/m² (5000-psig) helium gaseous environments at 951°K (1250°F). Creep rate, rupture life, percent elongation, and percent reduction of area were determined for one cast nickel-, two wrought nickel-, and one wrought cobalt-base alloys.

B. RESULTS AND CONCLUSIONS

Creep and rupture properties were degraded in 34.5-MN/m² (5000-psig) hydrogen at 951°K (1250°F) for the four alloys tested. Degradation in rupture life is expressed as percent reduction of life in hydrogen or hydrogen/water vapor compared to helium tested at same stress, temperature and pressure conditions, as shown in table VII-1. Stress-rupture curves are shown in figures VII-1 through VII-4.

Table VII-1. Degradation Based on Rupture Life

Alloys	Stress, MN/m ² ksi		Life Time to Rupture, hr			Degradation
			He	H ₂	H ₂ /H ₂ O	
Cast Nickel Base						
IN100	551	80	>140.0	1.6		99%
	620	90	7.6	0.2		97%
Wrought Nickel Base						
WASPALLOY [®] (AMS 5706)	607	88	58.2	25.1		57%
Astroloy	793	115	87.8	59.6		32%
Wrought Cobalt Base						
Haynes 188	365	53	80.3	43.2		46%
	483	70	9.4	5.4		42%
	365	53			55.5	31%
	483	70			6.3	33%

Note:

Degradation (Time to Rupture)

=

Time_{He}

-

Time_{H₂}

Time_{He}

X 100%

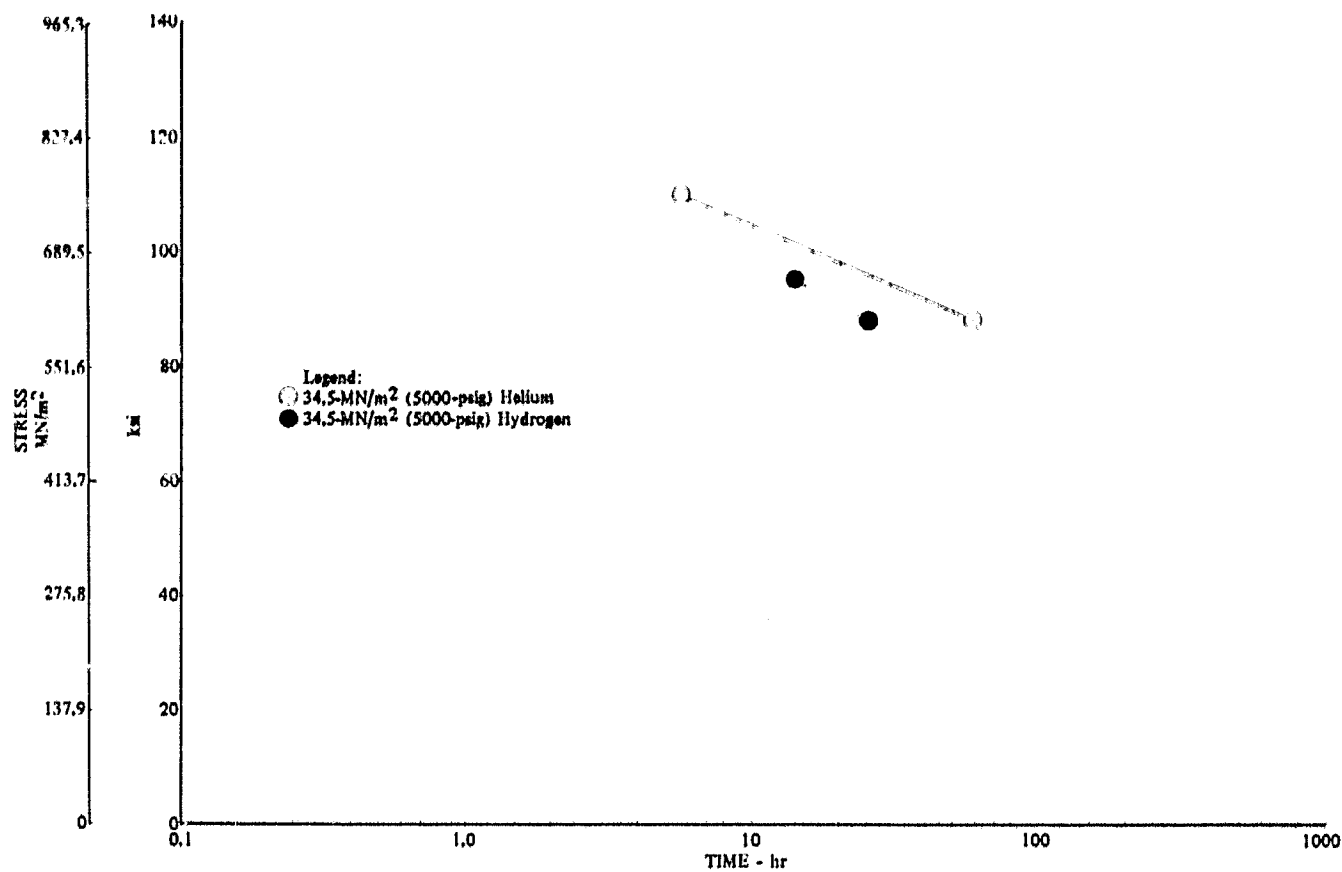


Figure VII-1. Stress Rupture of Waspaloy[®] (AMS 5706) at 951°K (1250°F) DF 91365

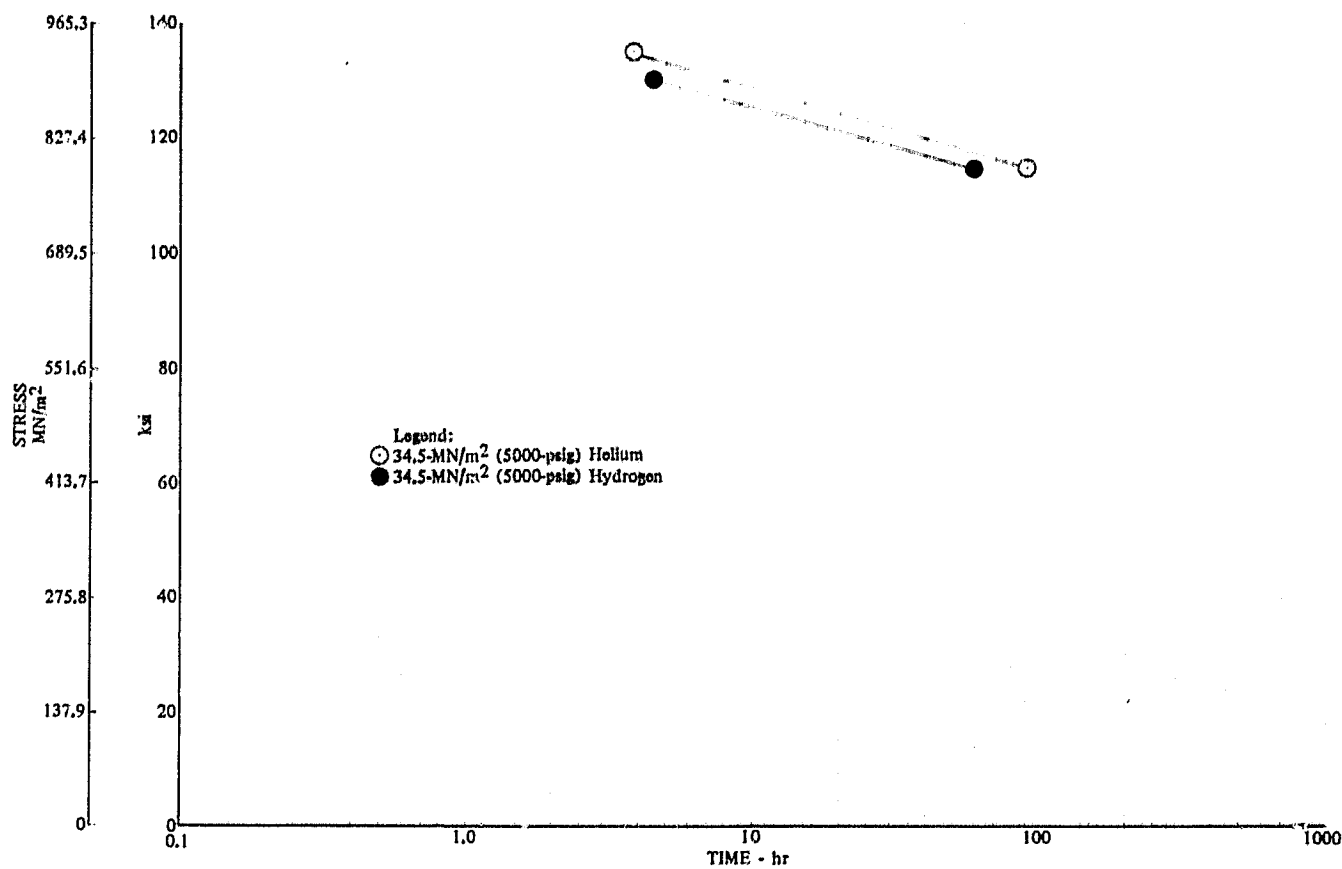


Figure VII-2. Stress Rupture of Astroloy at 951°K (1250°F) DF 91366

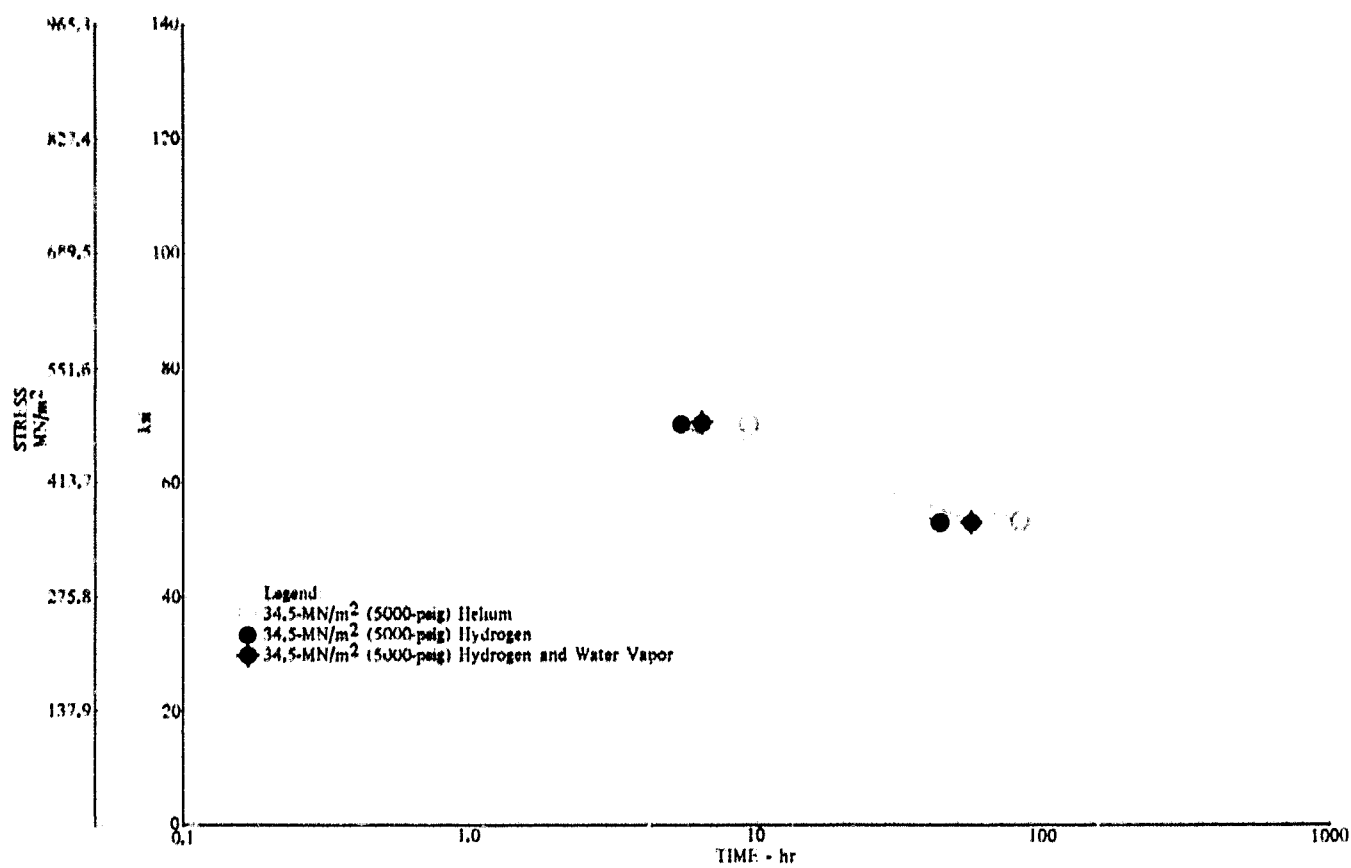


Figure VII-3. Stress Rupture of Haynes 188 at 951°K (1250°F) DF 91367

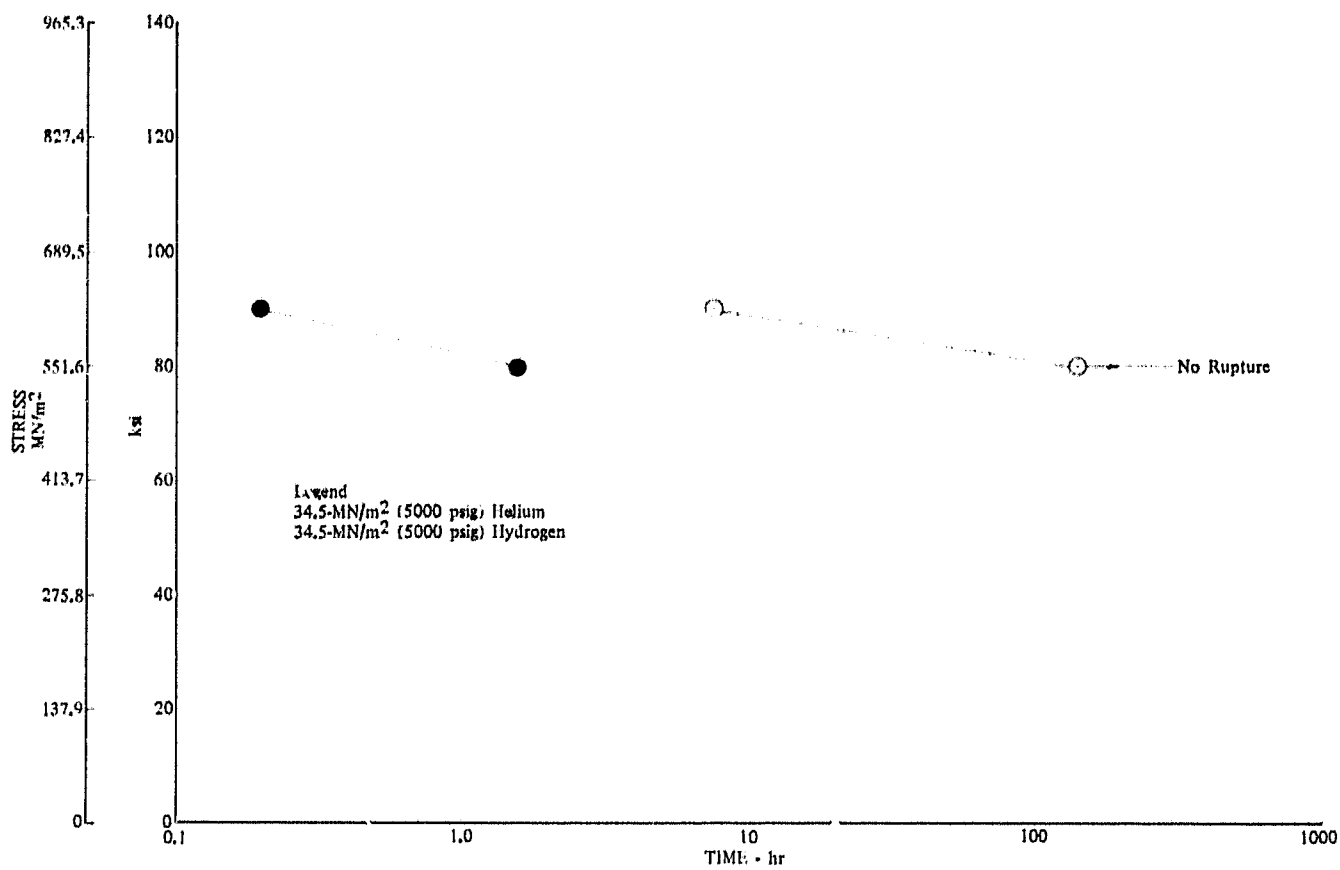


Figure VII-4. Stress Rupture of IN100 at 951°K (1250°F) DF 91368

The addition of water vapor to the pure hydrogen environment reduces the degradation of Haynes 188 by one-third. This indicates that water vapor in the operating environment of a hydrogen-oxygen system will act as an inhibiting agent for Haynes 188. As only one alloy and concentration of water vapor have been tested, the degree of degradation versus the amount of water vapor in the system, or a threshold level, could not be established. It is expected, that water vapor in the hydrogen would inhibit mechanical property degradation for these alloys.

Generally, creep rates were greater in hydrogen than helium for all alloys tested. Comparative creep-rate data are summarized below for 1% and 2% creep.

	Stress, MN/m ² ksi		Time (hr) to Creep (%) of:			
			1.0%		2.0%	
			He	H ₂	He	H ₂
Haynes 188	365	53	4.5	1.4	9.0	4.0
	483	70	0.7	0.4	1.5	0.9
Waspaloy (AMS 5706)	607	88	21.0	12.5	36.3	19.0
Astroloy	793	115	17.5	18.0	49.0	37.0
IN100	Less Than 0.5% Creep					

All creep-rupture failures in the wrought alloys exhibited the intergranular failure mode typical for rupture failures. All specimens also exhibited intergranular secondary cracking, except the Astroloy. In Astroloy specimens tested in both the helium and hydrogen, the primary failure was intergranular; however, in the hydrogen environment, the secondary cracking and cracking branching from the primary failure were transgranular. This is unusual for this type of alloy for stress-rupture tests at this temperature. A typical example of this transgranular cracking, which occurred in a hydrogen environment, is shown in figure VII-5. Comparative creep-rate curves are shown in figures VII-6 and VII-7 for AMS 5706 WASPALOY® and Astroloy, respectively, tested at 951°K (1250°F) in 34.5-MN/m² (5000-psig) hydrogen or helium. Complete data are given in table VII-2.

C. TEST PROCEDURE

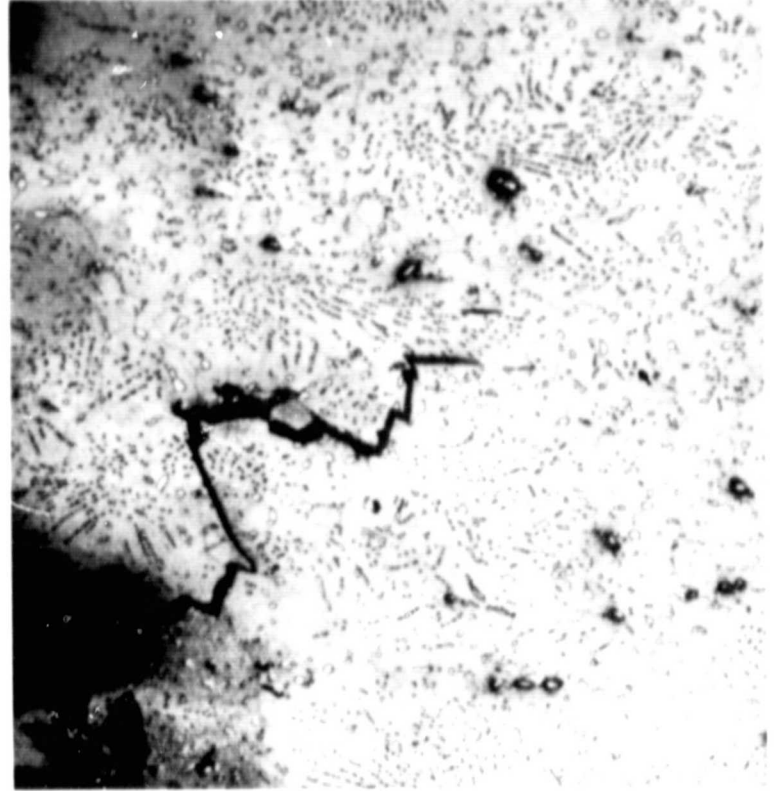
The creep-rupture tests in helium and hydrogen environments were conducted on a modified 12,000-lb capacity Arcweld Model JE creep-rupture machine. The test machine and test vessel were explosion-proofed and located in an enclosure exposed to atmospheric conditions. Controls and readout were located in an adjacent blockhouse. The pressure vessel was suspended in the creep-rupture machine, which was counterbalanced to maintain the load lever arm in a level position.

The creep-rupture specimen was designed and machined with integral collars for positive location and gripping of creep-measuring extensometer heads. The ends of the specimen are flat pin joints, rather than conventionally threaded joints, which act as part of a universal joint. Load rods and adapters also incorporate pin joints, which, in effect, put a universal joint at the immediate ends of the specimen, and minimize or eliminate alignment errors and resulting bending stresses upon the specimen.



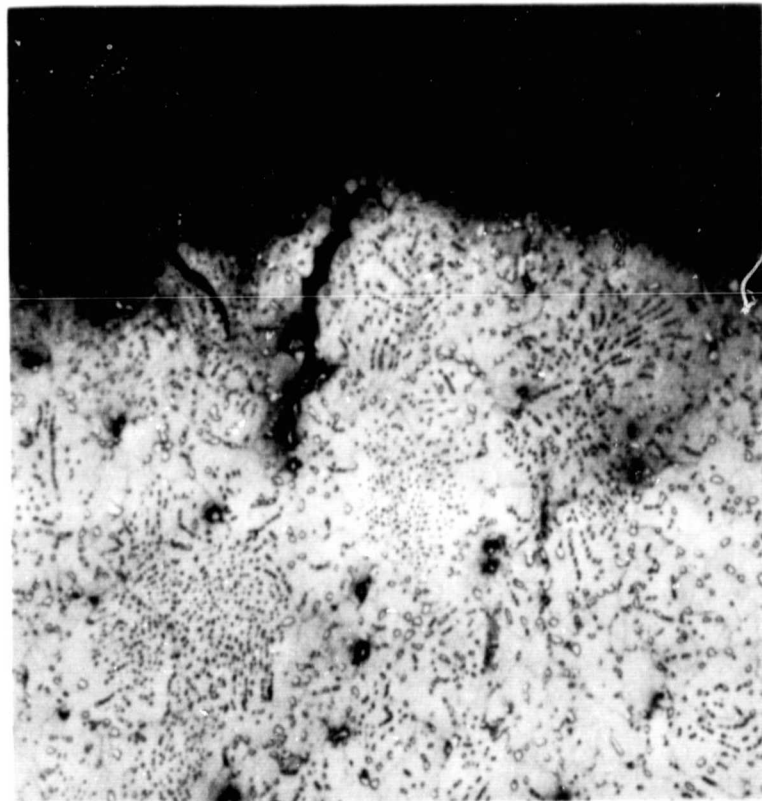
FAM 77187
Mag: 100X

Typical Grain Structure Duplex, ASTM 4-8 and 2-3



FAM 77158
Mag: 200X

Inter and Transgranular Secondary Crack



FAM 77160
Mag: 200X

Transgranular Cracks Progressing From Primary
Intergranular Failure



FAM 77159
Mag: 1000X

Enlargement of Inter and
Transgranular Secondary Crack

Figure VII-5. Micrographs From Gage Section of
an Astroloy Creep-Rupture Specimen
Tested at 951°K (1250°F) in 34.5-MN/m²
(5000-psig) Gaseous Hydrogen

FD 63048

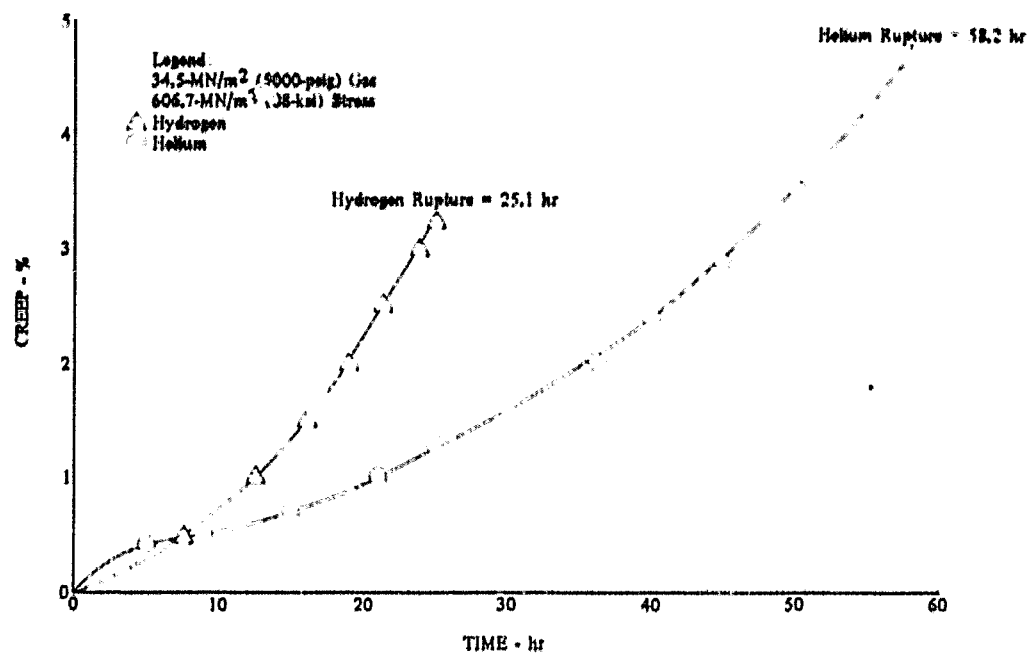


Figure VII-6. Creep-Rupture of Waspaloy^R (AMS 5706) at 951 °K (1250 °F) DF 91363

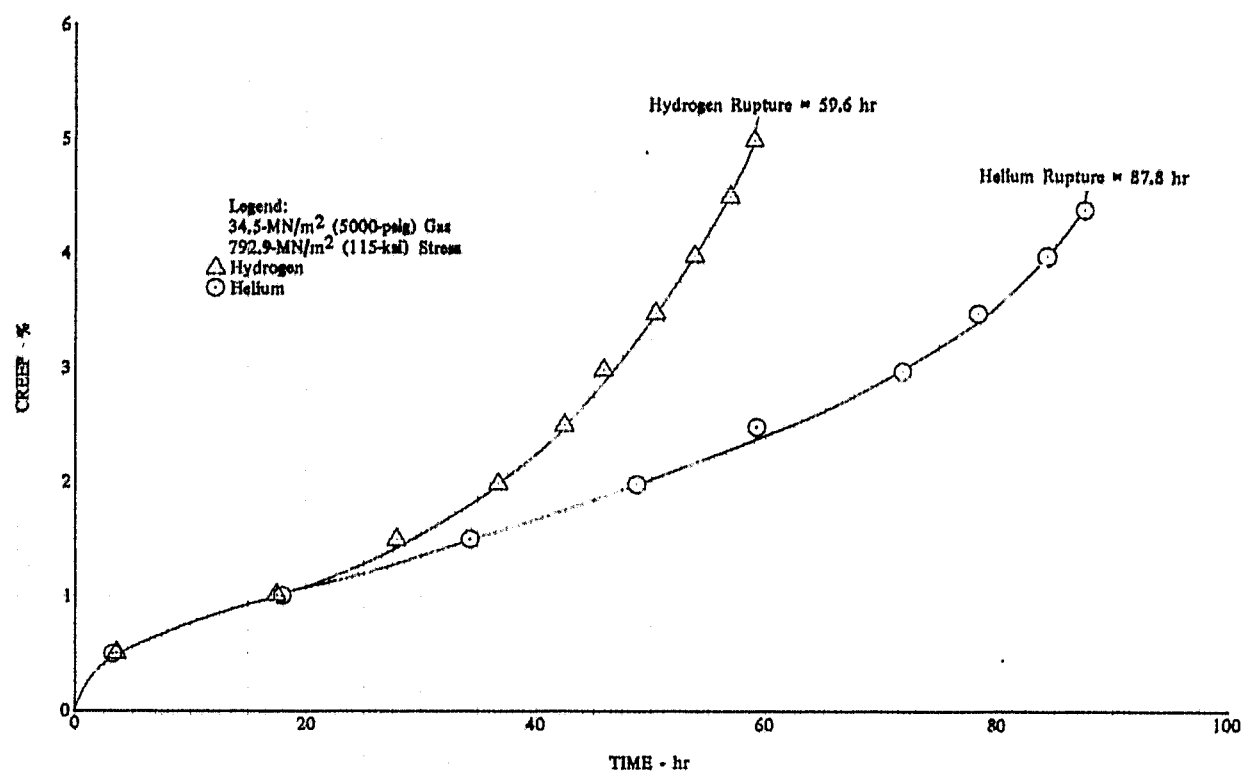


Figure VII-7. Creep-Stress Rupture of Astroloy at 951 °K (1250 °F) DF 81364

As the specimen ends were exposed to the high-pressure gas, a load-compensating technique eliminated any effective load on the specimen due to pressure. The extensometer was inside the vessel and was of the averaging type. The output of the extensometer was recorded as elongation versus time. A time-run meter validated the rupture life indicated on the strip chart.

The specimen heater was a resistance wire, split, clamshell configuration. Two zones were provided with independent control to enable correct temperature along gage length. Three chromel-alumel thermocouples were looped tightly around the gage section with ceramic beads. The split heater was positioned around the specimen and extensometer heads. The pressure vessel was closed and connected to load rod adapters in the creep-rupture machine. The gas pressure lines, water cooling lines, and electric power leads were connected, and a low-pressure leak check was performed with gaseous nitrogen. The pressure vessel was evacuated to 100 μ of mercury and pop-purged 10 times with test gas.

The vessel was pressurized to 4000-psig with the test gas and stabilized to check for high-pressure leaks. Temperature was applied to specimen and allowed to stabilize by adjusting the primary temperature controller. Temperature increased gas pressure, which was vented, as necessary, to maintain 5000 psig. Stable temperature and pressure were obtained in 1-1/2 to 2 hr. Test load was applied by activating the automatic lever arm leveling unit. Dead weights were lifted off the rest pan to a position where the lever arm was maintained in a level position. The correct load, compensating for frictional losses, was verified by the internal load cell. The test system was secured for automatic control and monitoring. When the specimen failed, all control equipment was automatically deactivated. The specimen was removed, and final gage length and diameter were measured and recorded to determine the percent elongation and percent reduction of area.

The procedure was modified for the hydrogen/water vapor tests. Water was initially processed to remove minerals and entrapped gases. This was accomplished by triple distillation, followed by reheating to the boiling point in pyrex bottle, with an immediate evacuation and sealing from the surrounding atmosphere.

Standard test procedure was followed through the point of final evacuation. Test gas was introduced to increase test vessel pressure above the critical pressure, but below atmospheric pressure. The water injection system was installed (figure VII-8). By sequencing the hand valves, the plumbing interconnecting the test vessel, a water supply bottle, and a low-pressure hydrogen supply (from same gas source as test gas) was evacuated. After the water injection system was evacuated, the hand valves were closed and opened in proper sequence to cause the low-pressure hydrogen to push the water into the pressure vessel. A pan near the top of the vessel collected the water. Furnace heat caused vaporization. The water injection system was shut off and removed. High-pressure test gas was introduced, and the standard test procedure was continued.

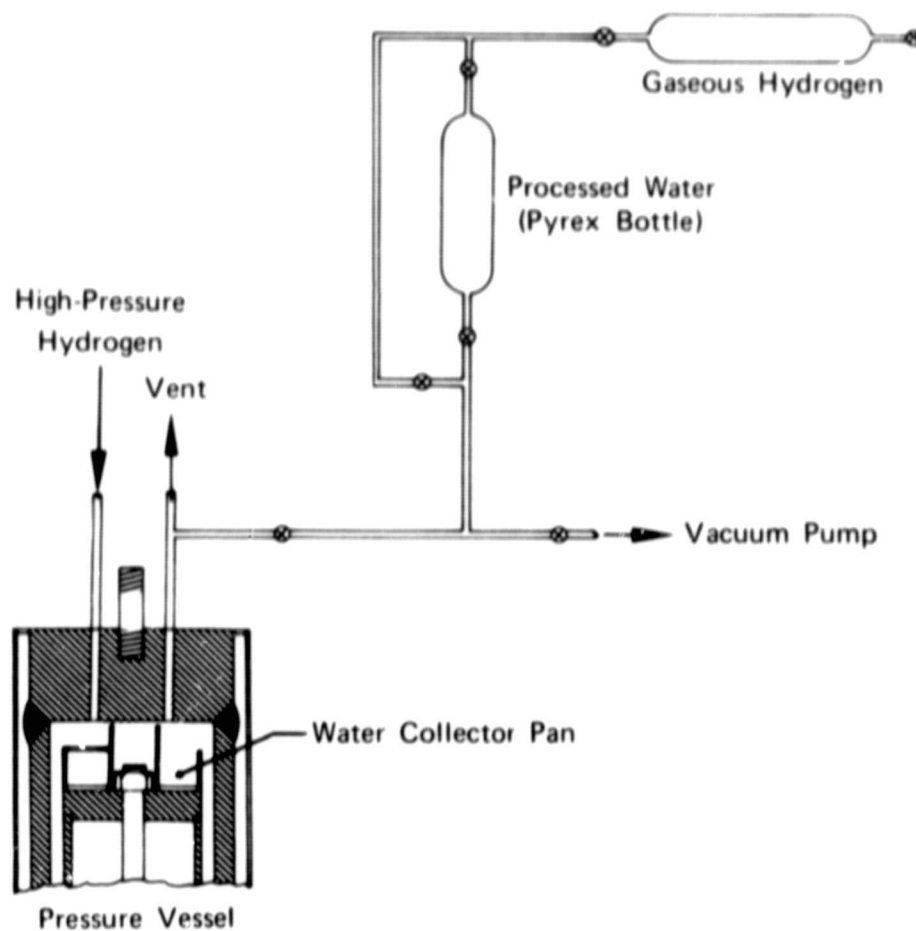


Figure VII-8. Creep-Rupture Water Injection System FD 63043

Within the limitations of the present test rig and test stand systems, no precise experimental method of determining the water content at test conditions of 34.5 MN/m^2 (5000-psi) and 951°K (1250°F) is possible. Analytical analyses of the system environment have established 30,000-ppm water vapor (3% by weight) for the equilibrium conditions present. This is the optimum available within the confines of the existing test rig and systems.

Table VII-2. Creep-Rupture Properties of Materials in High-Pressure Gaseous Environment

Test Results									
Test Conditions									
Material	Test Temperature,		Environ- ment	Pressure		Stress Level	Time to Creep,		Reduction of Area, %
	°K	°F		MN/m ²	psi		1.0% hr	2.0% hr	
IN100	951	1250	Helium	34.5	5000	551.6	80.0	<0.2% Total Creep	140.0(1)
	951	1250	Helium	34.5	5000	620.5	90.0	<0.3% Total Creep	7.6
	951	1250	Hydrogen	34.5	5000	620.5	90.0	<0.2% Total Creep	0.2
	951	1250	Hydrogen	34.5	5000	551.6	80.0	<0.5% Total Creep	1.6
Haynes 188	951	1250	Helium	34.5	5000	482.6	70.0	0.7	1.5
	951	1250	Helium	34.5	5000	365.4	53.0	4.5	9.0
	951	1250	Hydrogen	34.5	5000	365.4	53.0	1.4	4.0
	951	1250	Hydrogen	34.5	5000	482.6	70.0	0.4	0.9
	951	1250	Hydrogen/ Water Vapor	34.5	5000	365.4	53.0	No Measurement	55.5
	951	1250	Hydrogen/ Water Vapor	34.5	5000	482.6	70.0	No Measurement	6.35
	951	1250	Water Vapor	34.5	5000	482.6	70.0	No Measurement	21.2(2)
WASPALLOY®(AMS 5706)	951	1250	Helium	34.5	5000	758.4	110.0	2.0	3.9
	951	1250	Helium	34.5	5000	606.7	88.0	21.0	36.3
	951	1250	Hydrogen	34.5	5000	658.4	95.5	10.5	(3)
	951	1250	Hydrogen	34.5	5000	606.7	88.0	12.5	19.0
Astroloy	951	1250	Helium	34.5	5000	792.9	115.0	17.5	49.0
	951	1250	Helium	34.5	5000	930.8	135.0	No Measurement	3.8
	951	1250	Hydrogen	34.5	5000	896.3	130.0	1.5	3.3
	951	1250	Hydrogen	34.5	5000	792.9	115.0	18.0	37.0

Elongation is measured over 25.4-mm (1-in.) original gage length.

- Notes: (1) Did not fail, test discontinued
(2) Includes yielding upon loading
(3) 2.0% creep occurred during rupture
(4) Failure mode precludes accurate measurement

SECTION VIII TENSILE PROPERTIES

A. INTRODUCTION

Smooth or notched tensile tests were conducted on two cast and two wrought nickel-base alloys (MAR M-200 DS, IN100, WASPALOY[®], and Astroloy) to evaluate the tensile properties of these materials in 3.45-MN/m² (500-psi) or 34.5-MN/m² (5000-psi) gaseous helium and hydrogen atmospheres at room and elevated temperatures.

Tensile properties were determined for smooth specimens for all materials and for notched specimens ($K_t = 8.0$) of Astroloy only. Results of helium tests provided a baseline for comparison with hydrogen tests. Some Astroloy tensile tests were also conducted in air at atmospheric pressure to provide further comparisons.

B. CONCLUSIONS AND DISCUSSION

All the alloys evaluated in the tensile tests were nickel base, and all exhibited degradation of some property due to the hydrogen environment at one or more of the temperatures tested. The relative degree of hydrogen degradation is summarized in table VIII-1. It must be emphasized that the degradations listed in this table are based upon a limited amount of test data, and, therefore, can only indicate the trend of response of these alloys to the hydrogen environment and cannot be considered as absolute values.

The most severely degraded alloys were the MAR M-200 DS and the IN100, respectively, both cast alloys. The properties most affected by the hydrogen environment were the elongation and reduction of area, with as much as 75% decrease in ductility at room temperature. The degree of degradation of both alloys decreased with increasing temperature, with the IN100 significantly less susceptible to hydrogen degradation at 951°K (1250°F) than at room temperature.

The WASPALOY material was tested at 951°K (1250°F) only. It exhibited no degradation of yield and ultimate strength, or reduction of area. The only property that was degraded was the elongation. It is expected that WASPALOY would exhibit more degradation due to the hydrogen environment at lower temperatures, as this is the general trend with nickel-base alloys.

The MAR M-200 DS, IN100, and WASPALOY materials were tested in 34.5-MN/m² (5000-psig) gaseous helium and hydrogen. Bar charts comparing tensile properties of these alloys are shown in figures VIII-1 through VIII-3, respectively.

Table VIII-1. Relative Degradation of Tensile Properties of Materials in Gaseous Hydrogen Environment

Degradation (Change From Helium) ⁽¹⁾ In									
34.5-MN/m ² (5000-psig) Hydrogen Environment									
Material	Temperature, °K °F		0.2% Yield Strength	Ultimate Strength	Elongation	Reduction of Area	Ratio Of Ultimate Strengths (Hydrogen/Helium)	Ratio Of Notch/Smooth Ultimate Strength, Helium Hydrogen	
MAR M-200 DS (Smooth)	300	80	11%	-25%	-75%	-6%	0.75	-	-
	951	1250	None	-14%	-47%	-48%	0.86	-	-
IN100 (Smooth)	300	80	None	-18%	-71%	-70%	0.82	-	-
	951	1250	None	None	-12%	-17%	1.0	-	-
WASPALLOY® (Smooth)	951	1250	None	None	-17%	None	1.0	-	-
Astroloy (Notched)	300	80	-	-10%	-	-	0.90	1.21 ⁽³⁾	-
	951	1250	-	- 9%	-	-	0.91	-	-
	1144	1600	-	+11%	-	-	1.11	-	-
3.45-MN/m ² (500-psig) Hydrogen Environment									
Astroloy (Smooth)	951	1250	None	None	+ 5%	+12%	1.0	-	-
	1144	1600	+18%	+11%	+10%	+12%	1.11	-	-
Astroloy (Notched)	300	80	-	- 5%	-	-	0.95	1.21 ⁽³⁾	-
	951	1250	-	- 3%	-	-	0.97	1.25	1.22
	1144	1600	-	+ 6%	-	-	1.06	1.69	1.61

(1) Minus Signs Indicate Degradation in Hydrogen Environment. Plus Signs Indicate Improvement in Property in Hydrogen Environment
(2) None Indicates Less Than 3% Change in Property.
(3) Based on Smooth Ultimate Strength in Air at Ambient Pressure.

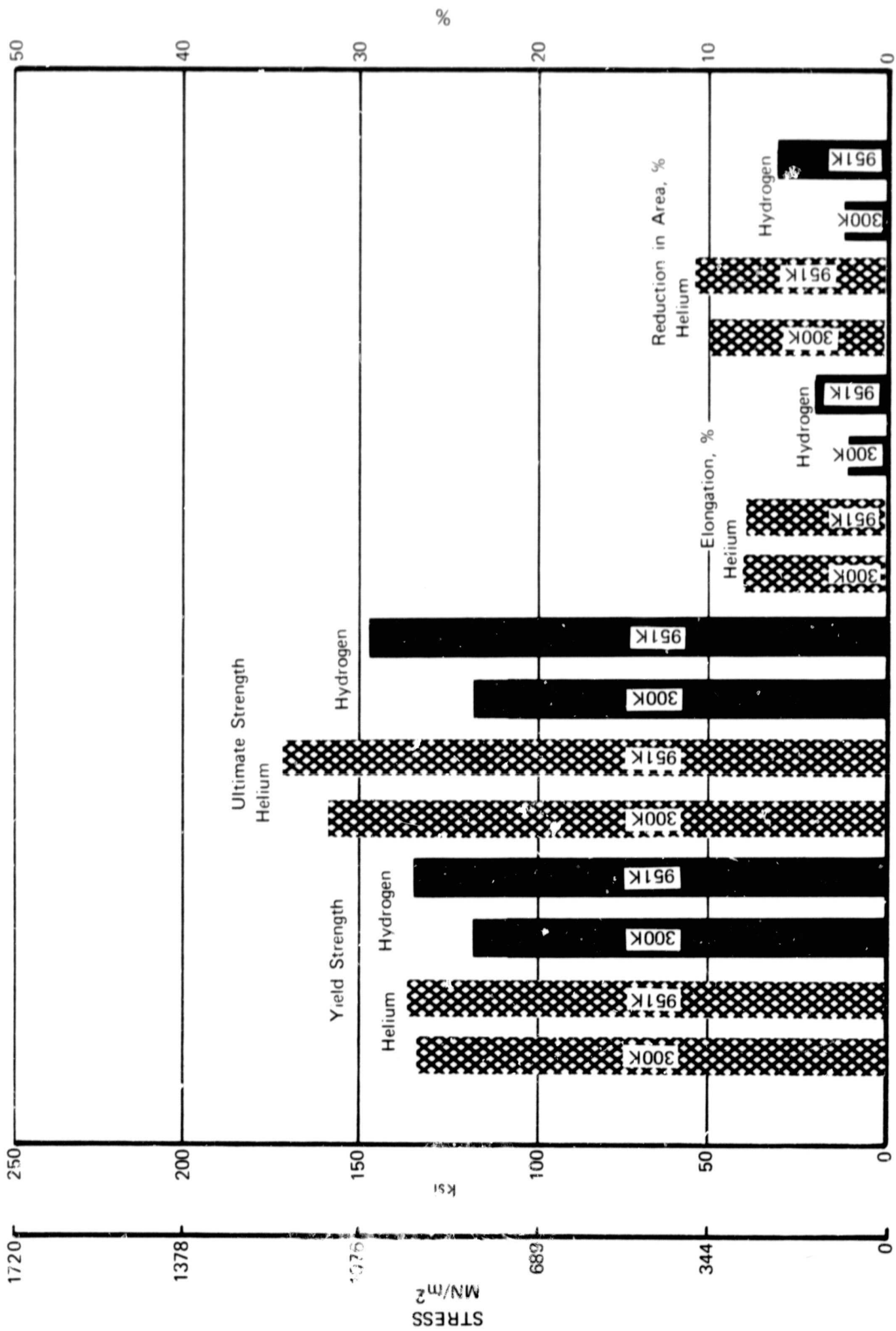


Figure VIII-1. Tensile Properties of MAR M-200 DS in 34.5-MN/m² (5000-psig) Gaseous Environment at 300°K (80°F) and 951°K (1250°F)

FD 62087

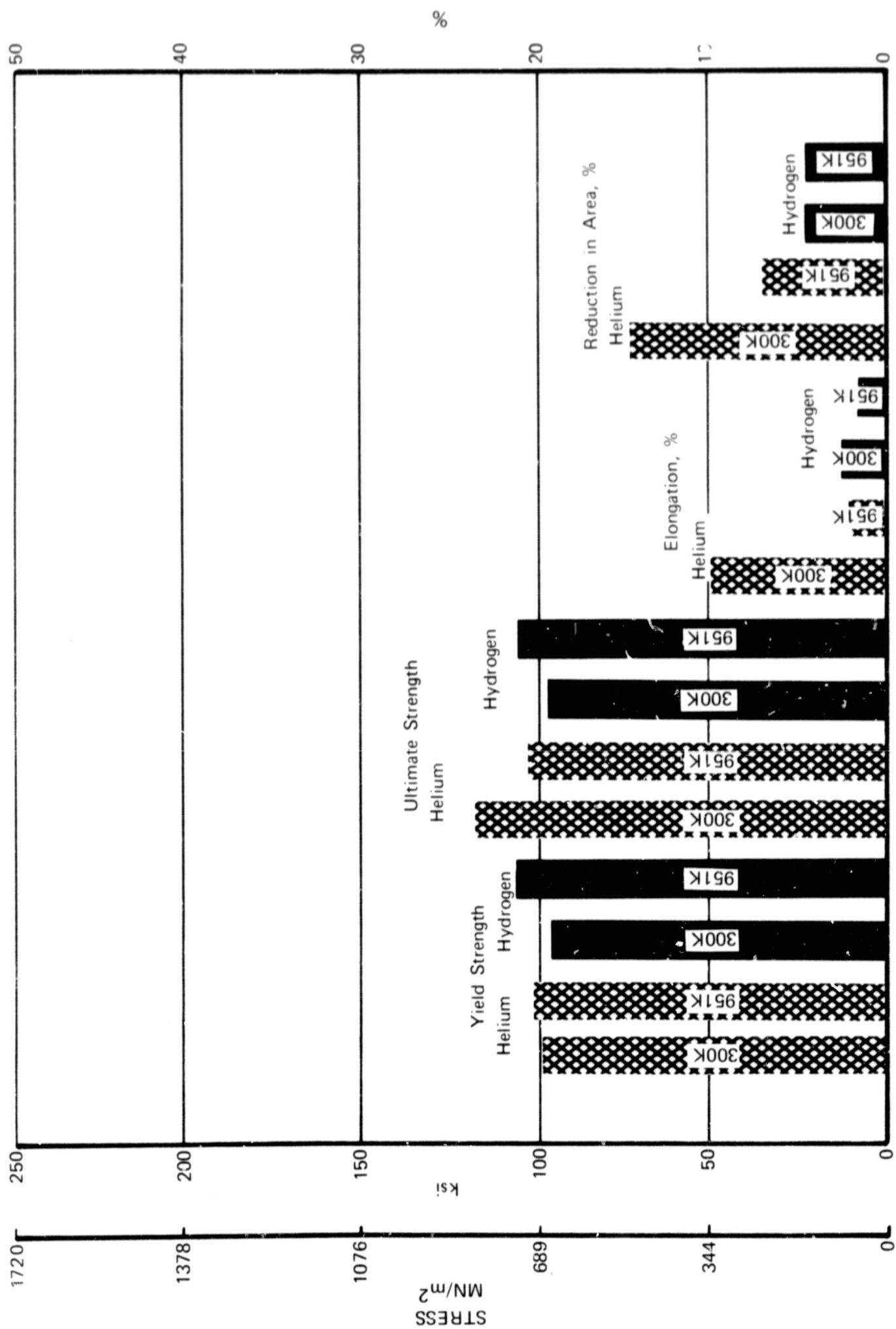


Figure VIII-2. Tensile Properties of IN100 in 34.5-MN/m² (5000-psig) Gaseous Environment at 300°K (80°F) and 951°K (1250°F)

FD 62088

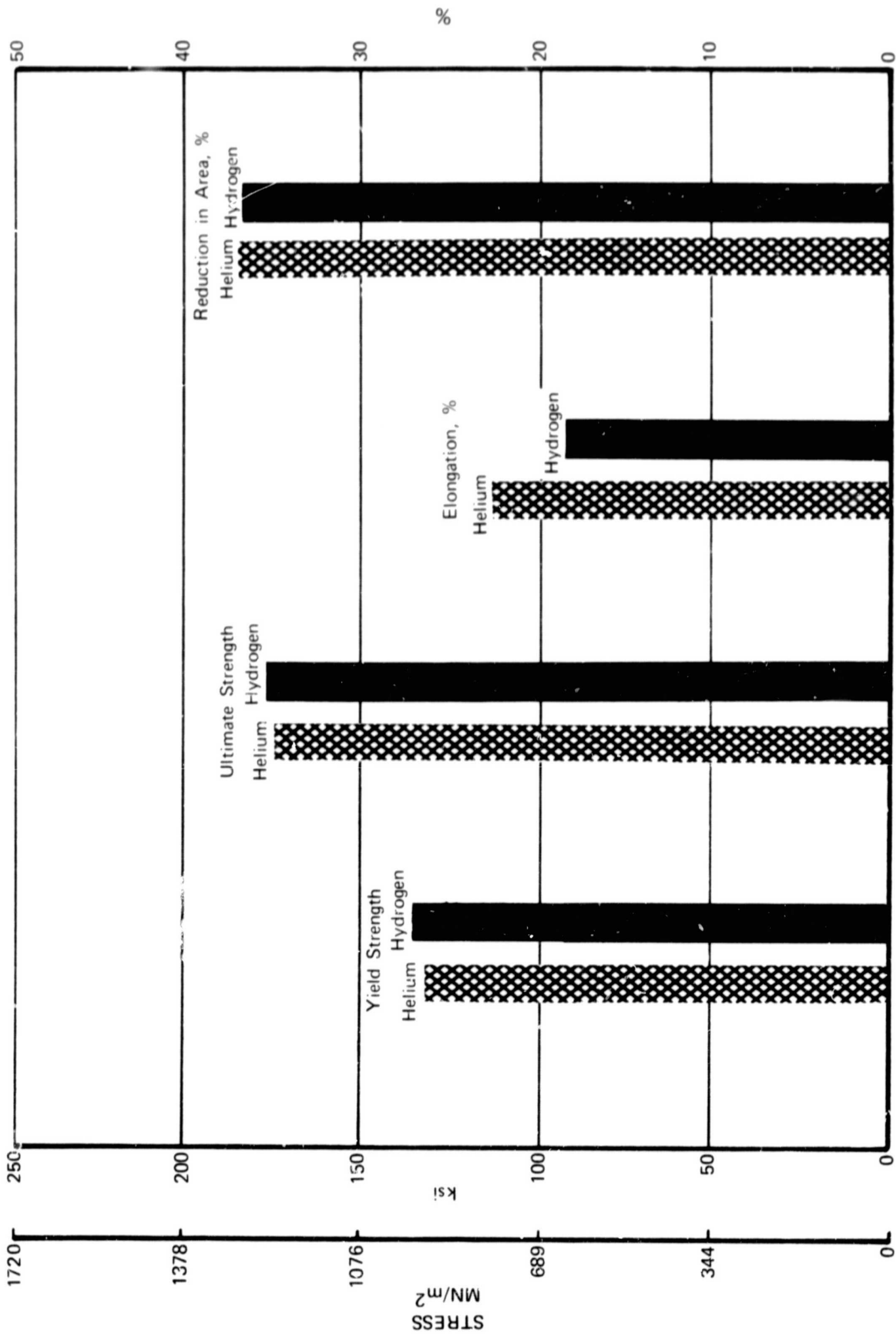


Figure VIII-3. Tensile Properties of WASPALOY[®] in 34.5-MN/m² (5000-psig) Gaseous Environment at 951°K (1250°F)

FD 62089

The Astroloy material was tested at two pressure levels, 3.45 and 34.5 MN/m² (500 and 5000 psig) and three temperatures, 300°, 951°, and 1144°K (80°, 1250°, and 1600°F). In addition, some tests were conducted in air at ambient pressure for comparison purposes. Notched ($K_t = 8.0$) tensile strength was most extensively evaluated, being determined at each of three temperatures at two pressures. Effects of the hydrogen environment were more pronounced at 34.5 MN/m² (5000 psig) than at 3.45 MN/m² (500 psig). At 34.5 MN/m² (5000 psig), notched tensile strength degradation was approximately twice that at 3.45 MN/m² (500 psig) for temperatures of 300° and 951°K (80 and 1250°F).

The effects of temperature on tensile properties of Astroloy are shown in figures VIII-4 through VIII-7. The general decrease in strength with increasing temperature was expected, as well as the decrease in amount of hydrogen degradation with increasing temperature. The reversal in properties at 1144°K (1600°F) (that is, higher properties in hydrogen than in helium) was not expected. Additional testing was conducted that verified this occurrence. Metallographic examination of failed specimens tested at 1144°K (1600°F) in helium and hydrogen could not provide definite reasons for this property reversal. Photomicrographs of specimens tested in helium and hydrogen are shown in figures VIII-8 and VIII-9. The specimens were similar in most respects: general structure, grain size, and percent recrystallization were the same; intergranular cracking and tearing at MC carbides occurred in both environments; cracking at grain boundary carbides occurred in both; and fine, aging, gamma prime particle dispersion, while not identical from specimen to specimen, was not considered significant enough to be a factor contributing to the different response in the different environments.

The most significant difference between the hydrogen and helium specimens was the occurrence of voids at large unsolutioned gamma prime particles, located completely within a grain. These intragranular voids, while not consistent from specimen to specimen, occurred only in specimens tested in the hydrogen environment and not in specimens tested in the helium environment. The significance of this difference is not understood. At elevated temperatures, particularly those temperatures above 1033°K (1400°F), several factors can contribute to the response of Astroloy (or other nickel-base alloys) in the helium and hydrogen environments. The hydrogen will disassociate from a molecular-to-atomic gas, with both the physical and chemical activity of the hydrogen atoms at a very high level; therefore, diffusion can proceed at a high rate. The 1144°K (1600°F) temperature is beyond the normal operating range for Astroloy. In fact, this temperature is in the range of the aging heat treatment temperatures, and structural changes can take place even during the short-time exposures of a tensile test, because of the high straining that is occurring. To explain this change in degree of degradation and, particularly, the reversal of helium and hydrogen properties at 1144°K (1600°F), a better understanding of the hydrogen-material interaction mechanism must be obtained.

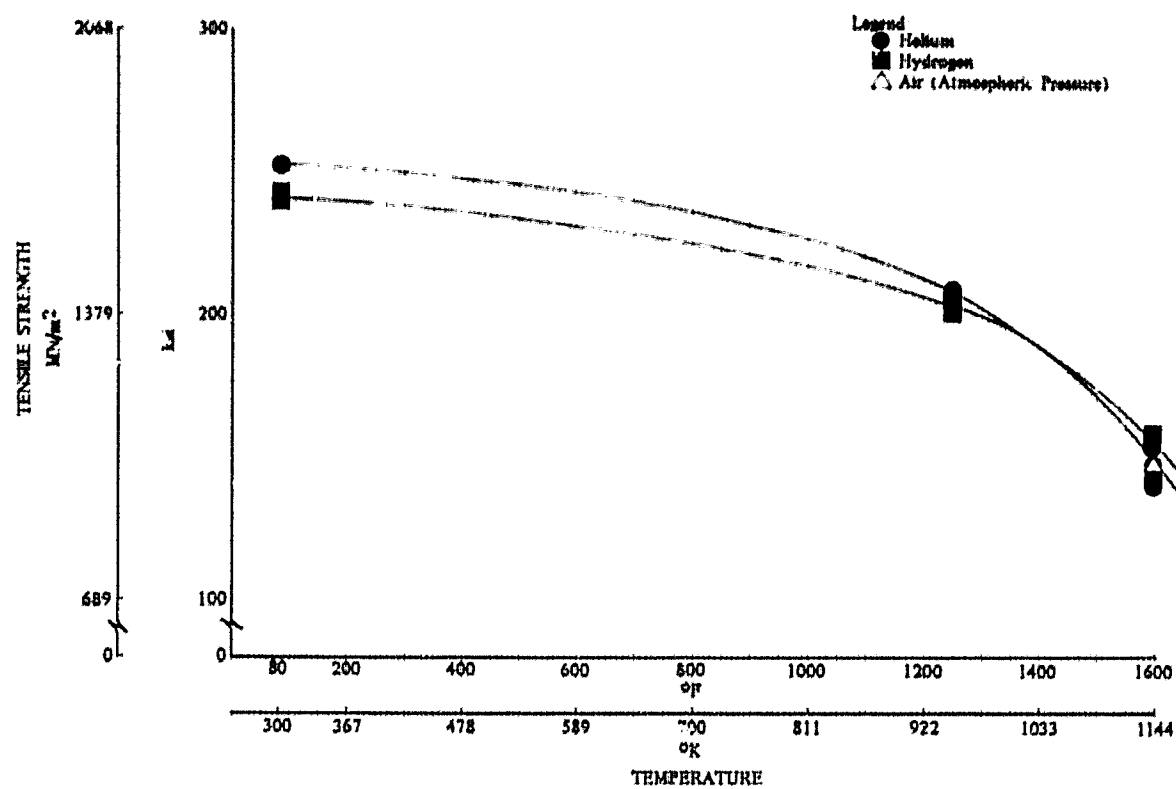


Figure VIII-4. Effect of Temperature on Notched ($K_t = 8.0$) Tensile Strength of Astroloy at 3.45 MN/m^2 (500 psig) DF 92136

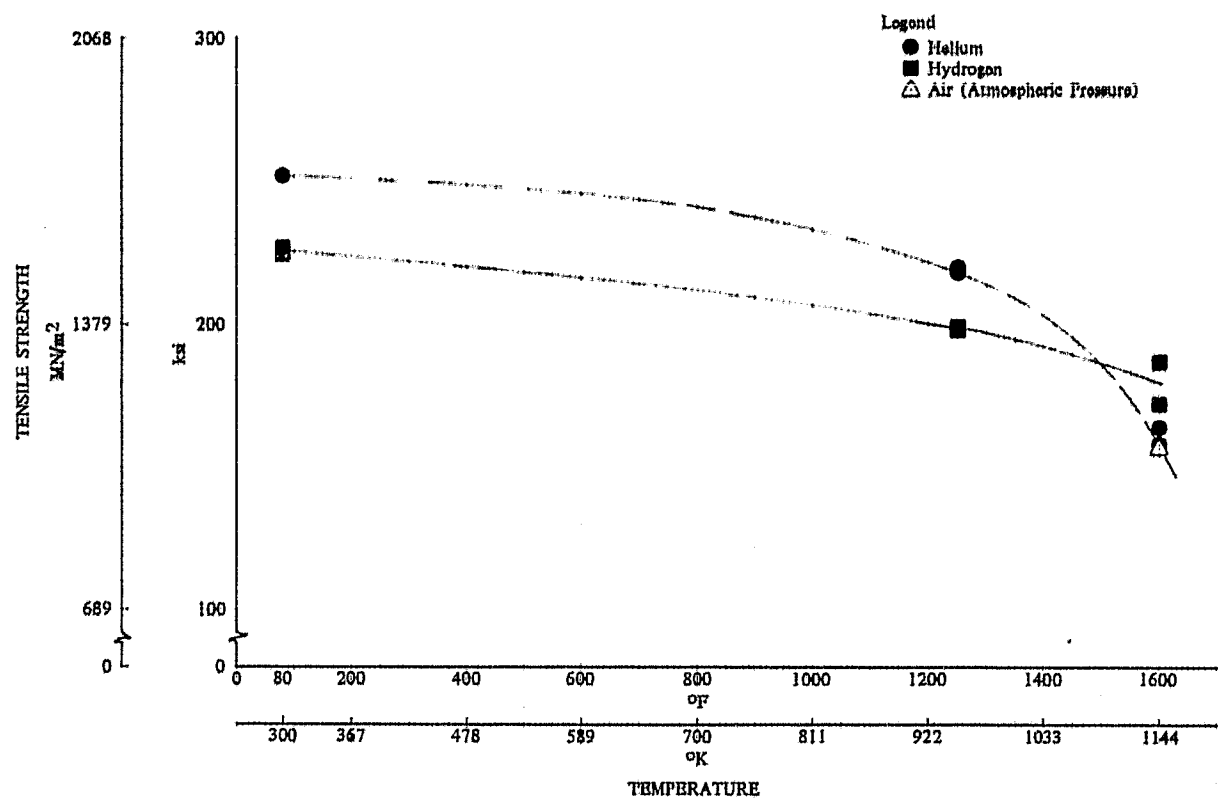


Figure VIII-5. Effect of Temperature on Notched ($K_t = 8.0$) Tensile Strength of Astroloy at 34.5 MN/m^2 (5000 psig) DF 92137

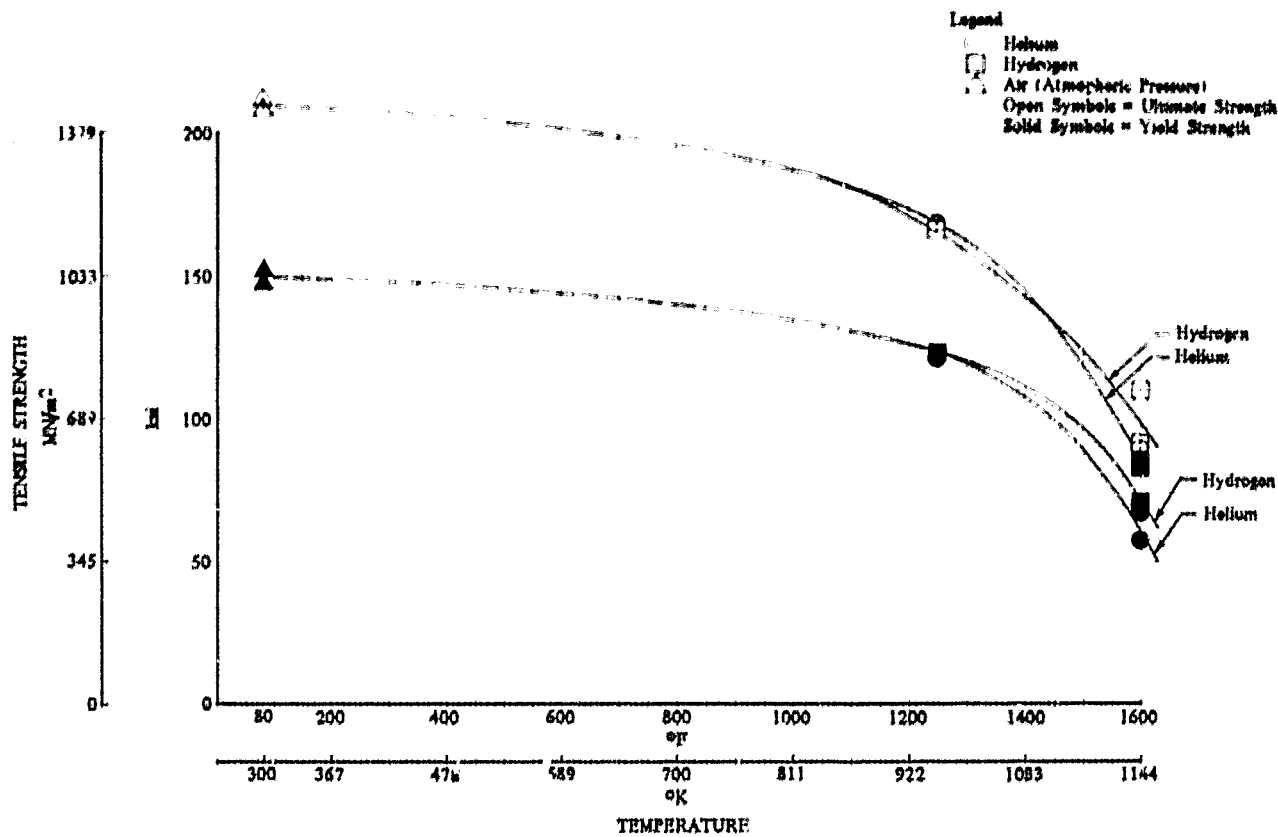


Figure VIII-6. Effect of Temperature on Smooth Tensile Yield and Ultimate Strength of Astroloy at 3.45 MN/m² (500 psig) DF 92138

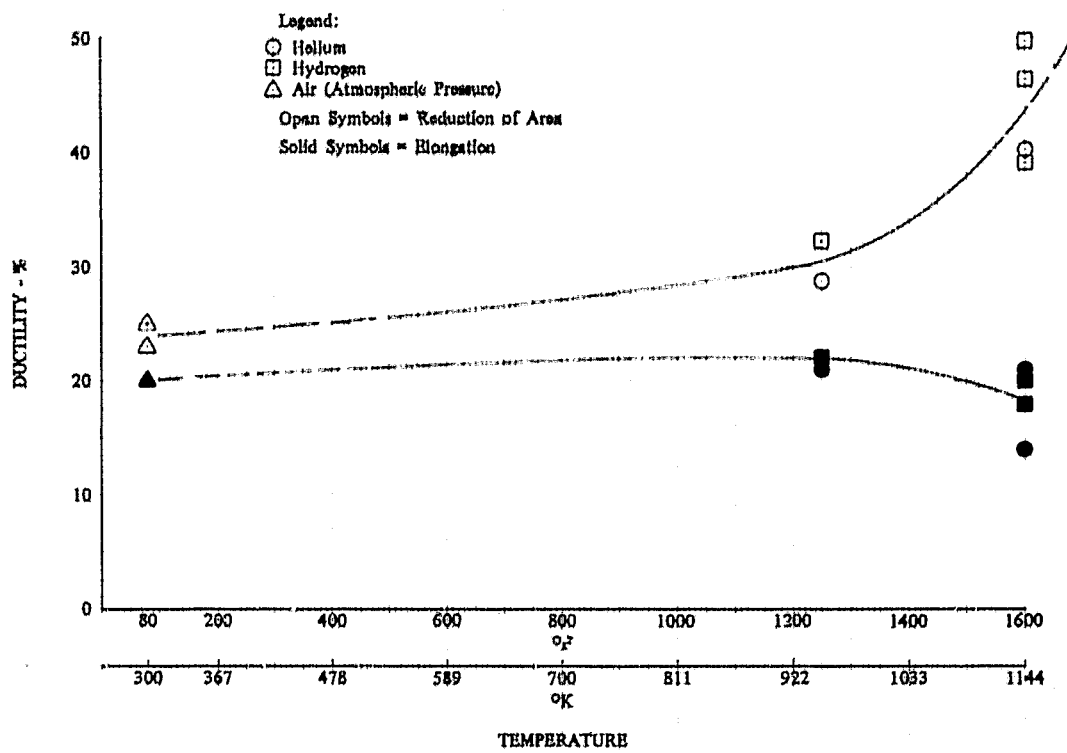
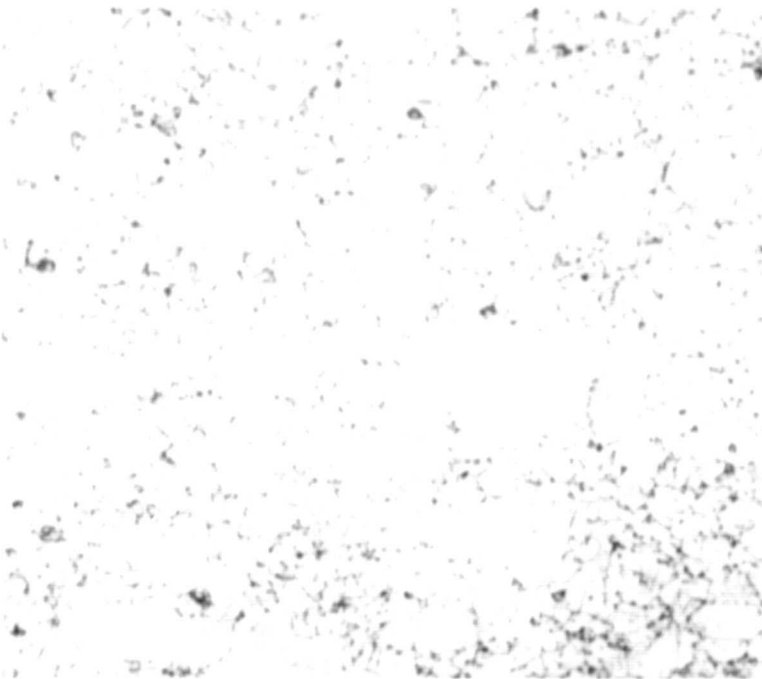
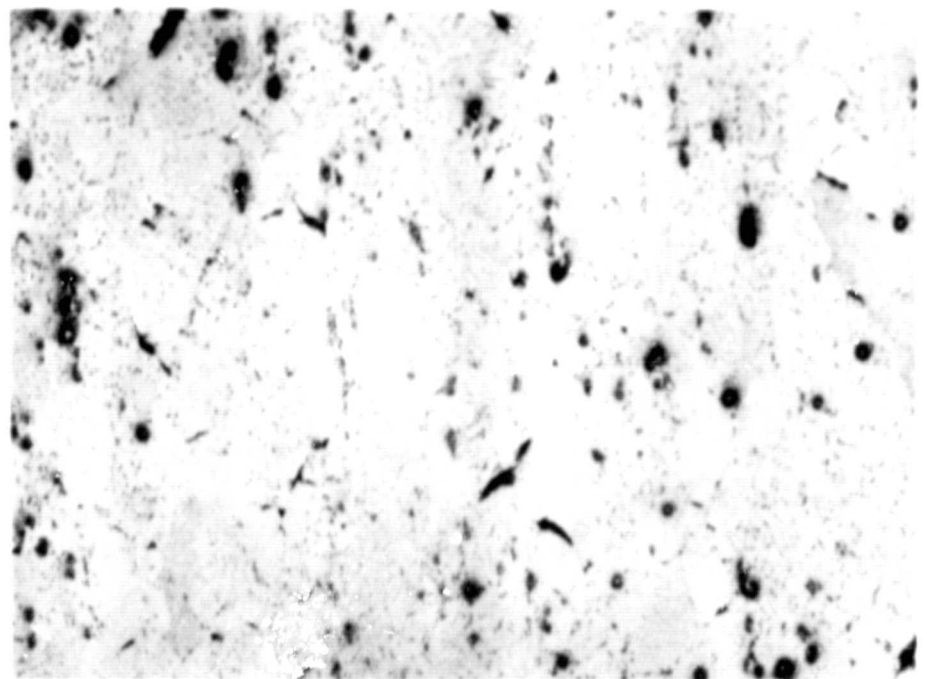


Figure VIII-7. Effect of Temperature on Smooth Tensile Ductility of Astroloy at 3.45 MN/m² (500 psig) DF 92139



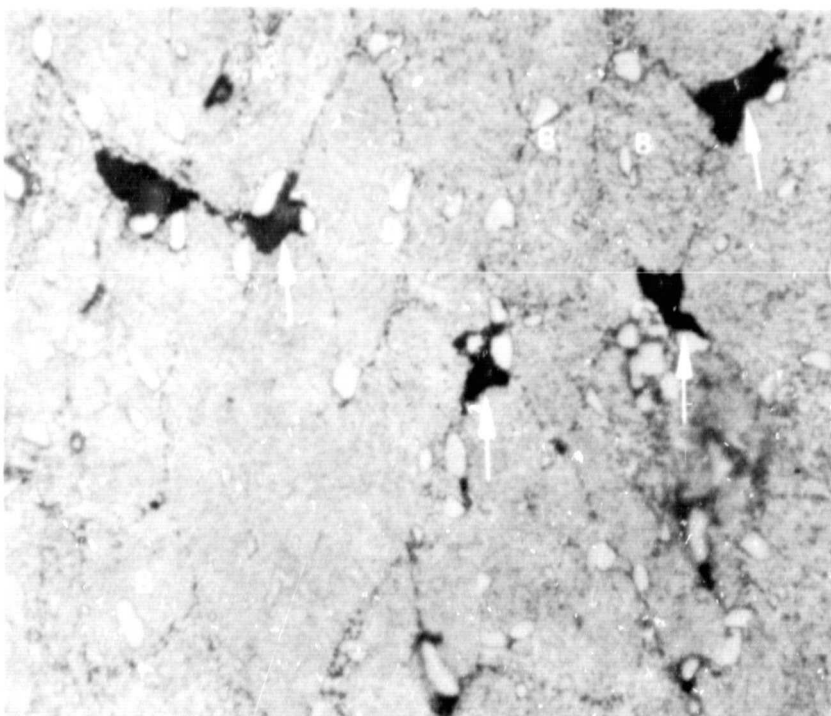
FAM 77194
Mag: 100X

Typical Grain Structure Duplex ASTM 5-8 and 3-4



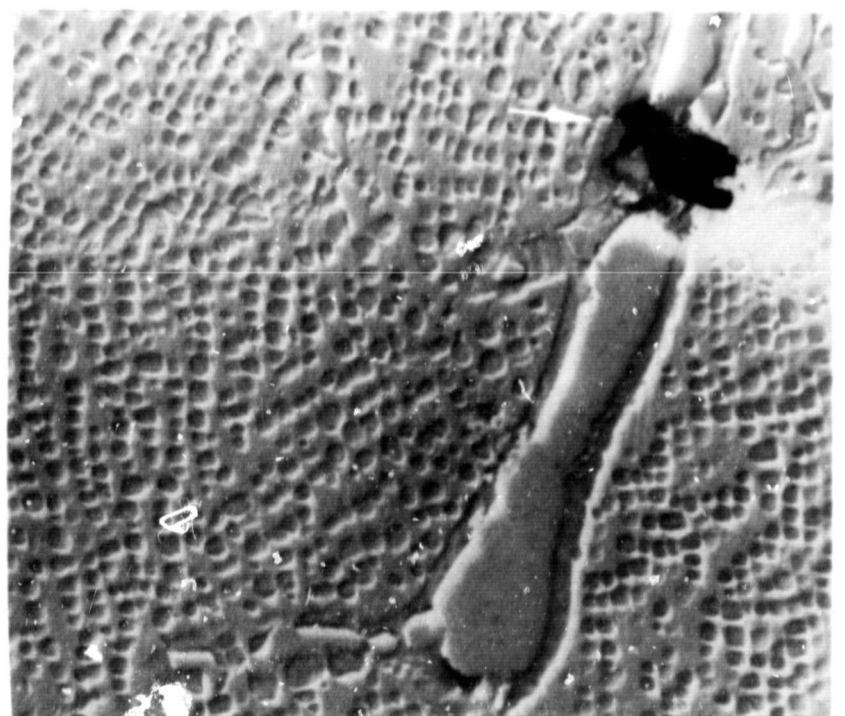
FAM 77166
Mag: 100X

Re-Etch Showing MC Carbides (A) With Tearing and Intergranular Cracks (↑)



FAM 77167
Mag: 1,000X

Enlargement Showing Large Gamma Prime Particles (B) and Intergranular Voids and Cracks (↑)

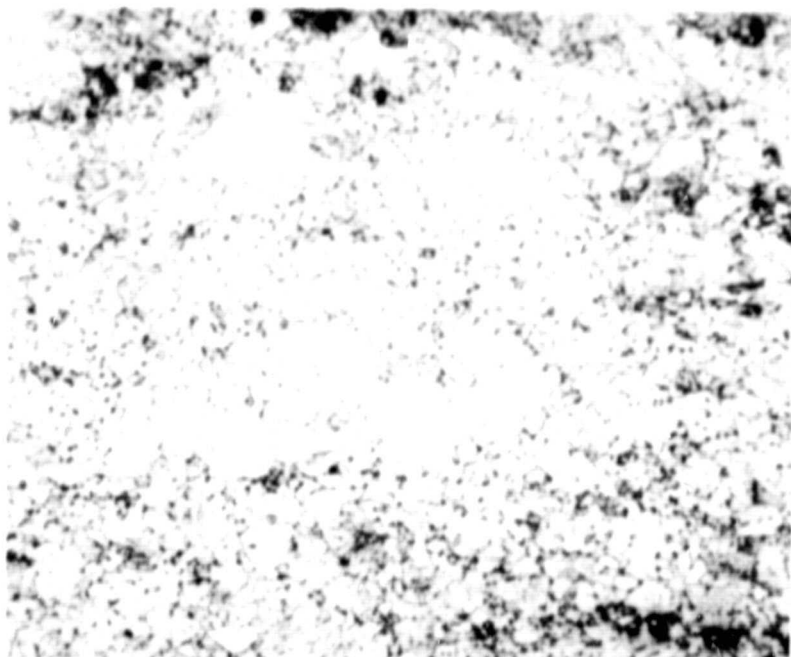


EM 4283-2
Mag: 10,000X

Electron Micrograph of Tearing at MC Carbide (↑)

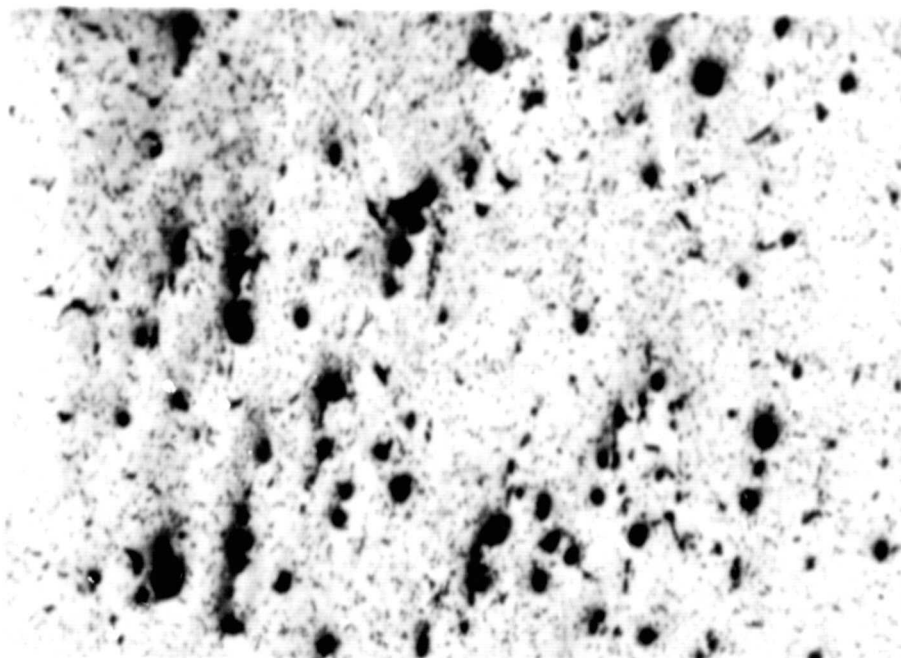
Figure VIII-8. Micrographs From Gage Section of an Astroloy Tensile Specimen Tested at 1144 °K (1600 °F) in 3.45-MN/m² (500-psig) Helium

FD 63046



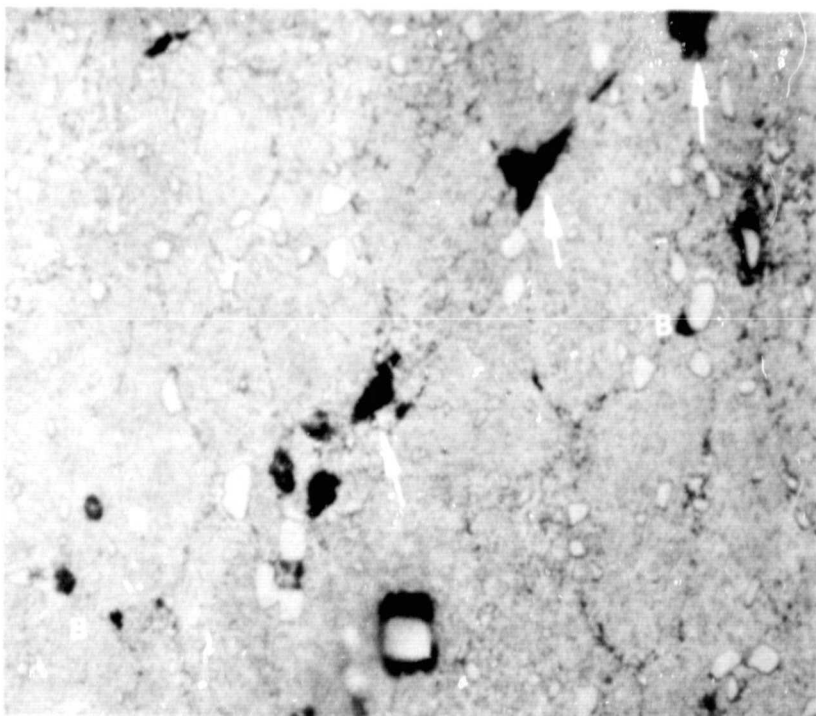
FAM 77196
Mag: 100X

Typical Grain Structure Duplex ASTM 5-8 and 4



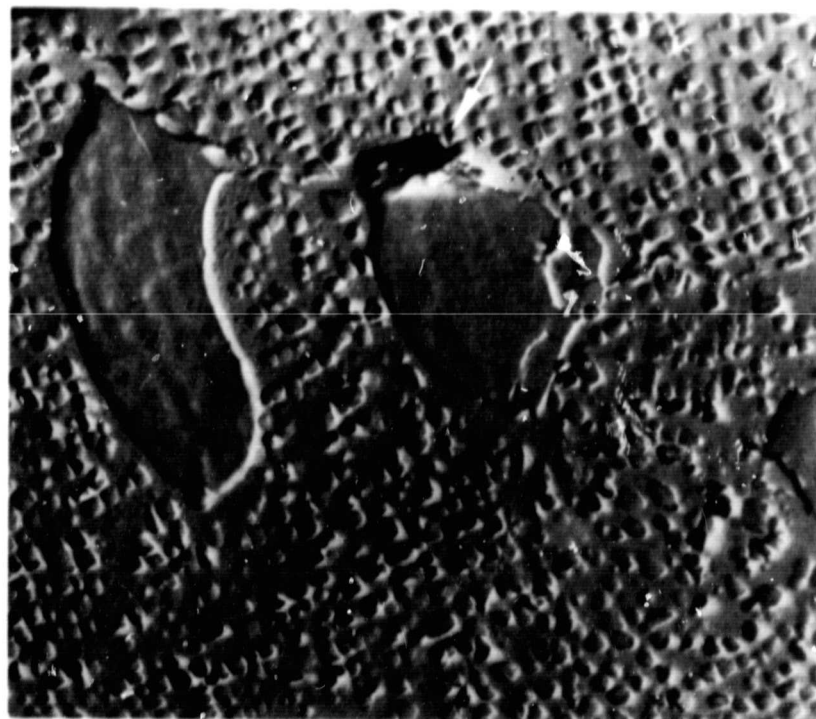
FAM 77164
Mag: 100X

Re-Etch Showing MC Carbides (A) With Tearing
and Intergranular Cracking (↑)



FAM 77165
Mag: 1000X

Enlargement Showing Large Gamma Prime Particles (B)
With Intragranular Voids and Intergranular Cracking (↑)



EM 4285-17
Mag: 10,000X

Electron Micrograph of Intragranular Void
at Large Gamma Prime Particle (↑)

Figure VIII-9. Micrographs From Gage Section
of an Astroloy Tensile Specimen
Tested at 1144°K (1600°F) in
3.45-MN/m² (500-psig) Hydrogen

FD 63047

C. TEST PROCEDURE

Two types of tensile specimens were used for this testing. All smooth round tensile specimens have a 6.40-mm (0.252-in.) gage diameter and a gage length of 25.4 mm (1.00 in.). Notched specimens (K_t of 8.0) have a larger diameter of 12.70 mm (0.500 in.) and a notch diameter of 8.00 mm (0.315 in.) machined in the center of the specimen gage at a 60-deg angle, with a 0.051 mm (0.002 in.) radius at the apex of the notch.

Tests conducted were essentially the same as those reported in PWA FR-4566. The Tinius-Olsen tensile machine was uprated to a 266.8-kN capacity, and the strain measuring system was converted to a proximity probe type similar to those systems in use for the creep-rupture and low-cycle fatigue tests. Specimen load was determined by both the tensile machine load measuring system and an internal strain gage-type load cell; thus, absolute specimen load was known and friction at the pressure vessel seals was of no consequence. Electrical connections to the internal load cell, extensometer, thermocouples and furnace were made through the bottom of the pressure vessel via high-pressure bulkhead connectors.

Elevated temperature testing was accomplished using a high-power density, two-zone furnace, with independent power supplies and controls mounted inside the pressure vessel. Thermocouples looped around the specimen gage section (or notch) were used to control and monitor specimen temperature during each test. Analyses of gas samples, before and after specimen tests, indicated required test gas purities were obtained.

Prior to each test, after specimen and instrumentation installation, the pressure vessel was evacuated several times and backfilled with nitrogen gas. The final system evacuation was to at least 50μ and was broken by the test gas. The vessel was then subjected to six test gas pop-purge cycles (described in Section IV) before test pressure was applied. When temperature and gas pressure were stabilized at the desired level, testing was conducted.

Tests of Astroloy at 34.5 MN/m^2 (5000 psig) and 1144°K (1600°F) were desired. For the helium environment, these conditions were obtained. For the hydrogen environment, the maximum obtainable pressure was limited by the thermal conductivity of the gas to 30.3 MN/m^2 (4400 psig) at 1144°K (1600°F). This was achieved by operating the furnace at the maximum power level available and venting pressure until a uniform, stable 1144°K (1600°F) specimen temperature was obtained. One helium test at 30.3 MN/m^2 (4400 psig) was then conducted for comparison purposes.

D. RESULTS

Ambient and elevated temperature test results are listed in table VIII-2 for all materials. Block diagrams showing relative hydrogen degradation at each temperature tested are given in figures VIII-1 through VIII-3 for MAR M-200 DS, IN100, and WASPALOY materials. Curves of notched and smooth tensile properties versus temperature of Astroloy at two pressures are plotted in figures VIII-4 through VIII-7.

END

Table VIII-2. Tensile Properties of Materials in High-Pressure Gaseous Environment

Test Conditions											
Material	Test Temperature		Stress Concentration Factor	Environment	Pressure		Strain Rate, %/min.		Strength		
	°K	°F			MM ²	PSI	0.005 Yld ¹	0.010 Yld ¹	MM ² Yld ²	KSI Yld ²	MM ² UTS ³
MAR M-200 DS	300	572	Smooth	Helium	34.5	5000	0.005	0.010	84.6	134.1	134.1
	300	572	Smooth	Hydrogen	34.5	5000	0.005	0.010	84.6	134.1	134.1
	300	572	Smooth	Helium	34.5	5000	0.005	0.010	84.6	134.1	134.1
	931	1708	Smooth	Helium	34.5	5000	0.005	0.010	84.6	134.1	134.1
	931	1708	Smooth	Hydrogen	34.5	5000	0.005	0.010	84.6	134.1	134.1
	931	1708	Smooth	Helium	34.5	5000	0.005	0.010	84.6	134.1	134.1
EN100	300	572	Smooth	Helium	34.5	5000	0.005	0.010	84.6	134.1	134.1
	300	572	Smooth	Hydrogen	34.5	5000	0.005	0.010	84.6	134.1	134.1
	300	572	Smooth	Helium	34.5	5000	0.005	0.010	84.6	134.1	134.1
	931	1708	Smooth	Helium	34.5	5000	0.005	0.010	84.6	134.1	134.1
	931	1708	Smooth	Hydrogen	34.5	5000	0.005	0.010	84.6	134.1	134.1
	931	1708	Smooth	Helium	34.5	5000	0.005	0.010	84.6	134.1	134.1
WASPALLOY ⁴	931	1708	Smooth	Helium	34.5	5000	0.005	0.010	84.6	134.1	134.1
	931	1708	Smooth	Hydrogen	34.5	5000	0.005	0.010	84.6	134.1	134.1
	931	1708	Smooth	Helium	34.5	5000	0.005	0.010	84.6	134.1	134.1
	931	1708	Smooth	Hydrogen	34.5	5000	0.005	0.010	84.6	134.1	134.1
	931	1708	Smooth	Helium	34.5	5000	0.005	0.010	84.6	134.1	134.1
	931	1708	Smooth	Hydrogen	34.5	5000	0.005	0.010	84.6	134.1	134.1
Astroloy	300	572	Smooth	Air	0	0	0.005	0.010	134.9	194.1	194.1
	300	572	Smooth	Helium	0	0	0.005	0.010	134.9	194.1	194.1
	300	572	Smooth	Hydrogen	0	0	0.005	0.010	134.9	194.1	194.1
	931	1708	Smooth	Helium	0	0	0.005	0.010	134.9	194.1	194.1
	931	1708	Smooth	Hydrogen	0	0	0.005	0.010	134.9	194.1	194.1
	931	1708	Smooth	Helium	0	0	0.005	0.010	134.9	194.1	194.1
	1244	2250	Smooth	Helium	0	0	0.005	0.010	134.9	194.1	194.1
	1244	2250	Smooth	Hydrogen	0	0	0.005	0.010	134.9	194.1	194.1
	1244	2250	Smooth	Helium	0	0	0.005	0.010	134.9	194.1	194.1
	1244	2250	Smooth	Hydrogen	0	0	0.005	0.010	134.9	194.1	194.1
	1244	2250	Smooth	Helium	0	0	0.005	0.010	134.9	194.1	194.1
	1244	2250	Smooth	Hydrogen	0	0	0.005	0.010	134.9	194.1	194.1
	1244	2250	Smooth	Helium	0	0	0.005	0.010	134.9	194.1	194.1
	1244	2250	Smooth	Hydrogen	0	0	0.005	0.010	134.9	194.1	194.1
	1244	2250	Smooth	Helium	0	0	0.005	0.010	134.9	194.1	194.1
	1244	2250	Smooth	Hydrogen	0	0	0.005	0.010	134.9	194.1	194.1
	1244	2250	Smooth	Helium	0	0	0.005	0.010	134.9	194.1	194.1
	1244	2250	Smooth	Hydrogen	0	0	0.005	0.010	134.9	194.1	194.1

¹ Elongation Measured Over 25.4-mm (1 in.) Original Gage Length.
² Strain Rate Does Not Apply to Nitrogen Environment.
³ Maximum Pressure Obtained at 1144-K (2087-F).